

Deuterated Polycyclic Aromatic Hydrocarbons in the Interstellar Medium: The Aliphatic C–D Band Strengths

DRAFT: 2023.8.9.55

X.J. Yang^{1,2} and Aigen Li²

ABSTRACT

Deuterium (D) was exclusively generated in the Big Bang and the standard Big Bang Nucleosynthesis (BBN) model predicts a primordial abundance of $D/H \approx 26$ parts per million (ppm). As the Galaxy evolves, D/H gradually decreases because of astration. The Galactic chemical evolution (GCE) model predicts a present-day abundance of $D/H \gtrsim 20$ ppm. However, observations of the local interstellar medium (ISM) have revealed that the gas-phase interstellar D/H varies considerably from one region to another and has a median abundance of $D/H \approx 13$ ppm, substantially lower than predicted from the BBN and GCE models. It has been suggested that the missing D atoms of $D/H \approx 7$ ppm could have been locked up in deuterated polycyclic aromatic hydrocarbon (PAH) molecules. However, we have previously demonstrated that PAHs with aromatic C–D units are insufficient to account for the missing D. Here we explore if PAHs with aliphatic C–D units could be a reservoir of D. We perform quantum chemical computations of the vibrational spectra of “superdeuterated” PAHs (in which one D and one H share an C atom) and PAHs attached with D-substituted methyl group, and derive the band strengths of the aliphatic C–D stretch ($A_{4.65}$). By applying the computationally derived $A_{4.65}$ to the observed aliphatic C–D emission at $\sim 4.6\text{--}4.8\ \mu\text{m}$, we find that PAHs with aliphatic C–D units could have tied up a substantial amount of D/H and marginally account for the missing D. The possible routes to generate PAHs with aliphatic C–D units are also discussed.

Subject headings: dust, extinction — ISM: lines and bands — ISM: molecules

¹Department of Physics, Xiangtan University, 411105 Xiangtan, Hunan Province, China; xjyang@xtu.edu.cn

²Department of Physics and Astronomy, University of Missouri, Columbia, MO 65211, USA; lia@missouri.edu

1. Introduction

A set of infrared (IR) emission features at 3.3, 6.2, 7.7, 8.6, and 11.3 μm , commonly attributed to polycyclic aromatic hydrocarbon (PAH) molecules, are ubiquitously seen in a wide variety of astrophysical environments. We should emphasize that astronomical PAHs are not necessarily *pure* aromatic compounds as strictly defined by chemists. Instead, PAH molecules in space may include ring defects, substituents, partial dehydrogenation, or superhydrogenation (see Yang et al. 2017 and references therein). Astronomical PAHs could also be deuterated (e.g., see Allamandola et al. 1989; Hudgins et al. 2004; Peeters et al. 2004; Draine 2006; Onaka et al. 2014, 2022; Mori et al. 2022; Yang et al. 2020, 2021). Indeed, it has been suggested that PAHs could be a reservoir of deuterium (D) in the interstellar medium (ISM; Draine 2006).

According to the standard Big Bang Nucleosynthesis (BBN) model, D was exclusively created in the Big Bang with a primordial D/H abundance of $[\text{D}/\text{H}]_{\text{prim}} \approx 26$ ppm (see Yang et al. 2020 and references therein). Due to astration (i.e., D is converted to ^3He , ^4He , and heavier elements in stellar interiors), the present-day Galactic interstellar D/H abundance should be reduced from the primordial abundance to $[\text{D}/\text{H}]_{\text{ISM}} \gtrsim 20$ ppm. However, the gas-phase $[\text{D}/\text{H}]_{\text{gas}}$ abundance of the local ISM derived from high resolution ultraviolet (UV) spectroscopic observations varies considerably from one region to another, and ranges from ~ 5 ppm to ~ 22 ppm, with a median abundance of $[\text{D}/\text{H}]_{\text{gas}} \approx 13$ ppm (see Draine 2006). This implies that there must exist a sink to accommodate the missing D/H, typically of ~ 7 ppm. The exact sink for the missing D atoms remains unknown. If PAHs are responsible for the missing D atoms, they should typically have tied up an amount of $[\text{D}/\text{H}]_{\text{PAH}} \approx 7$ ppm. Here $[\text{D}/\text{H}]_{\text{PAH}}$ refers to the amount of D locked up in PAHs (relative to the total H in the ISM).

If interstellar PAHs are deuterated through replacing one or more of their peripheral hydrogen (H) atoms by D atoms, one expects to see an emission band at $\sim 4.4 \mu\text{m}$, arising from the aromatic C–D stretch, in analogy to the 3.3 μm C–H stretch. Indeed, the 4.4 μm C–D stretching emission band has been detected in photodissociated regions (PDRs), reflection nebulae, and H II regions both in the Milky Way and in the Large and Small Magellanic Clouds (Peeters et al. 2004; Onaka et al. 2014, 2022; Doney et al. 2016). The intrinsic band strengths of the 4.4 μm C–D stretch have been computed by Yang et al. (2020, 2021) and Buragohain et al. (2015, 2016, 2020) and have been applied to astronomical observations to estimate the degree of D enrichment in PAHs. Yang et al. (2020, 2021) have found that small interstellar PAHs could indeed be D-enriched, exceeding the interstellar D/H abundance by a factor of $\gtrsim 1000$. Nevertheless, this is still not sufficient to account for the missing D atoms.

As will be discussed in §4.3, PAHs could also be deuterated by attaching D-containing

aliphatic sidegroups (e.g., $-\text{CH}_2\text{D}$) to their edge carbon (C) atoms, with the asymmetric and symmetric aliphatic C–D stretching modes occurring at $\sim 4.6\text{--}4.8\ \mu\text{m}$ (see Tielens 1997). Indeed, these C–D emission bands have also been seen in interstellar sources, together with the $4.4\ \mu\text{m}$ aromatic C–D stretch (Peeters et al. 2004; Onaka et al. 2014, 2022; Doney et al. 2016). In regions rich in H and D atoms, PAHs could be superhydrogenated by inserting an extra H atom to an edge C atom so that two H atoms share one C atom. This converts aromatic C–H stretches to aliphatic. In analogy, an D atom could also be squeezed in the peripheral, originally aromatic C–H unit to create an aliphatic C–H unit and an aliphatic C–D unit.

The goal of this work is to evaluate the role of PAHs containing aliphatic C–D units as a potential reservoir of D atoms. To this end, we first perform quantum chemical computations of the vibrational spectra of PAHs with deuterated aliphatic sidegroups and “superdeuterated” PAHs in which one H atom and one D atom share one C atom. The computational methods and target PAH molecules are summarized in §2. The computed spectra as well as the aliphatic C–D band strengths derived from the computed spectra are presented in §3. In §4.1 we compile all the astronomical data for the aliphatic C–D stretch. In §4.2 we apply the aliphatic C–D band strengths derived here to astronomical observations. We quantitatively determine the amount of D atoms possibly locked up in PAHs with aliphatic C–D units. The possible routes for aliphatically deuterating PAHs in the ISM are discussed in §4.3. Finally, we summarize our major results in §5. This paper is largely concerned with the quantum chemical computations of PAHs containing aliphatic C–D units. Readers who are interested only in the aliphatic C–D band intensities and the astrophysical applications may wish to proceed directly to §3.4.

2. Computational Methods and Target Molecules

We use the Gaussian16 software (Frisch et al. 2016) to calculate the IR vibrational spectra for different parent PAH molecules containing aliphatic C–D units. We consider seven parent aromatic molecules, i.e., benzene (C_6H_6), naphthalene (C_{10}H_8), anthracene ($\text{C}_{14}\text{H}_{10}$), phenanthrene ($\text{C}_{14}\text{H}_{10}$), pyrene ($\text{C}_{16}\text{H}_{10}$), perylene ($\text{C}_{20}\text{H}_{12}$), and coronene ($\text{C}_{24}\text{H}_{12}$). Here we focus on small PAHs with fewer than 24 C atoms (i.e., $N_{\text{C}} \lesssim 24$) since deuterium enrichment in PAHs of $N_{\text{C}} \gtrsim 40$ is not expected. Large PAHs have a sufficiently large number of internal degrees of freedom to accommodate the maximum energy of typical UV photons without subsequent photolytic bond cleavage occurring (Hudgins et al. 2004). Nevertheless, if the deuteration of PAHs occurs in D-enriched ice mantles through D-atom addition (see below), large PAHs could also be deuterated.

We consider PAHs with two categories of aliphatic C–D units, i.e., PAHs attached with one deuterated methyl group (hereafter PAH-CH₂D; see Figure 1) and “superdeuterated” PAHs (hereafter PAH-HD; see Figure 2) in which one edge C atom is shared by one H atom and one D atom. For both categories, various isomers are considered. As H is much more abundant than D, if a PAH molecule is “superdeuterated”, it is very likely that it will also be superhydrogenated (i.e., two H atoms share one C atom). Therefore, we consider “superdeuterated” PAHs to be superhydrogenated as well.

In dense regions where dust grains are coated by an ice mantle, upon condensation onto the ice mantle and exposed to UV irradiation, PAHs could be deuterated if interstellar ice is appreciably deuterated. Laboratory studies have shown that UV photolysis of PAHs in D-enriched ices results in rapid D enrichment of PAHs through aromatic D→H exchange, D-atom addition (“superdeuteration”), and exchange through keto-enol tautomerism (see Figure 4 of Sandford et al. 2000). The latter two reactions could also occur in the absence of UV irradiation. For illustrative purpose, we therefore also consider a deuterated molecule with a ketone (C=O) bond and a deuterated molecule with a deuteroyl (OD) sidegroup, using coronene as an example (see Figure 2).

To examine the effects of ionization on the vibrational spectra and aliphatic C–D band strengths of deuterated PAHs containing aliphatic C–D units, we also consider the cationic counterparts of “superdeuterated” PAHs (i.e., PAH-HD). For simplicity, we only consider PAHs with a single H and D pair (see Figure 3). They are essentially the radical counterparts of those molecules shown in Figure 2, with one H atom stripped off from their H and H pair.

In view of the fact that, observationally, the aliphatic C–D emission at ~ 4.6 – $4.8 \mu\text{m}$ is always seen together with the aromatic C–D emission at $\sim 4.4 \mu\text{m}$ (Peeters et al. 2004; Onaka et al. 2014, 2022; Doney et al. 2016), we also consider PAHs with both aromatic and aliphatic C–D bonds, taking pyrene as an example. We consider pyrenes in which an D atom substitutes an H atom *and* a deuterated methyl group (–CH₂D) is also attached (hereafter PyreD-CH₂D; see Figure 4). We also consider mono-deuterated pyrenes which are “superdeuterated” as well (hereafter PyreD-HD; see Figure 5). Again, as D is much less abundant than H, “superdeuterated” pyrenes are very likely also superhydrogenated. Different isomers are considered, with D atoms and functional groups attached at different positions.

We will refer PAHs with deuterated methyl sidegroups (see Figure 1) by the abbreviation of the first four letters of the names of their parental PAH molecules, followed by the position where the methyl group is attached and then “MD” (e.g., Naph1_MD refers to naphthalene with a deuterated-methyl group attached at position 1). For “superdeuterated” PAHs with an H and D pair as well as an H and H pair (see Figure 2), we use the abbreviation as

following: the first four letters of the names of their parental molecules followed by “2H” and then the order of the isomer followed by “HD” (e.g., Naph2H_2HD refers to the second isomer of superhydrogenated, superdeuterated naphthalene). For “superdeuterated” PAH cations (see Figure 3), we will also refer them by the abbreviation of the first four letters of the names of their parental molecules, followed by the position where the D atom is inserted and then “HD+” (e.g., Naph1_HD+ refers to naphthalene cation with the H and D pair attached at position 1). For deuterated pyrenes attached with CH₂D (see Figure 4), we use “Pyre” followed by the position where the methyl group is attached and then a letter of “D” followed by the position of the aromatic C–D bonds (e.g., Pyre1_D3 refers to pyrene with the deuterated-methyl group attached at position 1 and another D atom attached at position 3). For deuterated pyrenes which are also “superdeuterated” (see Figure 5), we use “Pyre2H” followed by the position where the H and D pair is attached, followed by “HD” and then “D” which is further followed by the position of the aromatic C–D bonds (e.g., Pyre2H_1HD_D3 refers to superdeuterated pyrene with the H and D pair attached at position 1 and another D atom attached at position 3).

We employ the hybrid density functional theoretical method (B3LYP) at the 6-311+G** level, which gives sufficient calculational accuracies with operable computer time (see Yang et al. 2017 and reference therein). The standard scaling is applied to the frequencies by employing a scale factor of ~ 0.9688 (Borowski 2012). We should note that the aromatic C–D band strengths of deuterated PAHs derived by Yang et al. (2020, 2021) from B3LYP/6-311+G** computations are consistent with recent laboratory measurements of deuterated quenched carbonaceous composites (Mori et al. 2022).¹

3. Vibrational Spectra and Aliphatic C–D Band Strengths of Deuterated PAHs

3.1. PAHs Attached with a D-substituted Methyl Group

For PAHs attached with a D-substituted methyl group (i.e., PAH-CH₂D), we calculate the vibrational spectra of 18 isomers of seven parent PAH molecules (see Figure 1), including all the possible positions where the methyl group is attached. Since each of the three H atoms in the methyl group (–CH₃) could be substituted with an D atom, therefore in total we consider 54 isomers.

¹The DFT-computed intensity ratio of the 4.4 μm aromatic C–D stretch to the 3.3 μm aromatic C–H stretch is $\approx 0.56 \pm 0.19$ for mono-deuterated PAHs (Yang et al. 2020) and $\approx 0.56 \pm 0.03$ for multi-deuterated PAHs (Yang et al. 2021), while the experimentally measured ratio is $\approx 0.56 \pm 0.04$ (Mori et al. 2022).

For each parent molecule, we obtain the mean spectrum averaged over all the isomers and show in Figures 6a–g. For each vibrational transition, we assign a width of 4 cm^{-1} . A feature at $\sim 2170\text{ cm}^{-1}$ (i.e., $\sim 4.61\ \mu\text{m}$), originating from aliphatic C–D stretches, is clearly seen in all these mean spectra. Also prominent are aliphatic and aromatic C–H stretches at $\sim 2980\text{ cm}^{-1}$ (i.e., $\sim 3.36\ \mu\text{m}$) and 3060 cm^{-1} (i.e., $\sim 3.30\ \mu\text{m}$), respectively. A close inspection of the aliphatic C–D stretches shown in Figures 6a–g reveals two or three peaks, attributed to different isomers. Nevertheless, these peaks are very close to each other, indicating that the centroids of the C–D stretches do not vary much among different isomers. As a matter of fact, the other vibrational modes are not significantly blended either, indicating that the transition frequencies for different isomers and different molecules are very similar, i.e., neither the position of the methyl group attached nor the position of D atoms in the methyl group affects the centroids of the vibrational features much.

Figure 6h shows the overall mean spectrum obtained by averaging over the mean spectra of all seven parent molecules (normalized by N_C). Again, the aliphatic C–D and C–H stretches are clearly seen, while the aromatic C–H stretch is the most prominent. The aliphatic C–D stretch also narrowly peaks, implying that the centroids of the C–D stretches do not vary much among different molecules. As the C–D in-plane and out-of-plane bending modes are often well mixed with the C–H out-of-plane bending modes and the C–C–C skeletal vibrational modes and therefore difficult to identify (Yang et al. 2020, 2021), we shall focus on the C–D and C–H stretching modes.

We tabulate the peak wavelengths and intensities of the C–H and C–D stretch features in Table 1. The aliphatic C–D stretches generally occur at $\sim 4.60\ \mu\text{m}$ and the deviation is negligible. In Figure 7 we show the intensities of the aliphatic C–D stretches ($A_{4.65}$), the aliphatic C–H stretches ($A_{3.4}$), and the aromatic C–H stretches ($A_{3.3}$) for all 54 isomers calculated here. The intensities of these stretches, especially the aromatic C–H stretches, show small scatters among different isomers. For aliphatic C–D stretches, the scatters mostly arise from the different positions of D atoms in the methyl group attached to the parent molecule. As D atoms substitute H atoms in the methyl group in a random manner, we should average the intensities over that for the three positions of the D atoms in the methyl group. This should also be the case for the methyl group attached at different positions of a parent molecule. Nevertheless, the scatters in the average intensities among the different isomers of the same parent molecule are small (see Table 1). The overall mean band intensities, on a per C–D or C–H bond basis, are $\langle A_{4.65} \rangle \approx 12.9 \pm 0.89\text{ km mol}^{-1}$, $\langle A_{3.4} \rangle \approx 23.1 \pm 1.3\text{ km mol}^{-1}$, and $\langle A_{3.3} \rangle \approx 14.3 \pm 1.1\text{ km mol}^{-1}$, respectively for the aliphatic C–D stretch, the aliphatic C–H stretch, and the aromatic C–H stretch.

3.2. “Superdeuterated” PAHs

The superhydrogenation of PAHs often starts from the broken of a C=C bond, followed by the addition of a pair of two H atoms in the neighbouring C atoms. By “superdeuterated” PAHs (PAH_{HD}), we refer to superhydrogenated PAHs but with one of the H atoms in the H and H pair substituted by an D atom, not two D atoms share one C atom. As mentioned earlier, H is much more abundant than D in space, if a PAH molecule is “superdeuterated”, it is very likely that it will also be superhydrogenated. Therefore, for “superdeuterated” PAHs we consider them to have a pair of two H atoms sharing an C atom, and meanwhile a pair of H and D atoms sharing another C atom. In total, we consider 24 isomers for seven parent molecules (see Figure 2).

For each parent molecule, we obtain the mean spectrum by averaging over the isomers (see Figures 8a–g). We also obtain the overall mean spectrum by averaging over all seven parent molecules (see Figure 8h). The aliphatic C–D stretches are clearly seen at $\sim 2150 \text{ cm}^{-1}$ (i.e., $\sim 4.65 \mu\text{m}$) and exhibit multiple peaks, indicating that the wavelengths of the aliphatic C–D stretches somewhat differ from one isomer to another.

The wavelengths and intensities of the C–H and C–D stretching transitions calculated for superdeuterated PAHs are tabulated in Table 2 and shown in Figure 9. Similar to PAHs attached with a D-substituted methyl group (PAH_{CH₂D}), the scatters in intensities are quite small among isomers and parent molecules, especially for the aromatic C–H stretch. The aliphatic C–D stretches of superdeuterated PAHs are more intense and peak at longer wavelengths than that of PAH_{CH₂D}, with $\langle \lambda_{\text{peak}} \rangle \approx 4.66 \mu\text{m}$ and $\langle A_{4.65} \rangle \approx 16.2 \text{ km mol}^{-1}$ for superdeuterated PAHs, while $\langle \lambda_{\text{peak}} \rangle \approx 4.60 \mu\text{m}$ and $\langle A_{4.65} \rangle \approx 12.9 \text{ km mol}^{-1}$ for PAH_{CH₂D}.

To investigate the effects of ionization on the vibrational spectra, we calculate the spectra for “superdeuterated” PAH cations (PAH_{HD}⁺). We consider the situation that only one C atom on the edge is superhydrogenated and attached with a pair of H and D atoms. We consider seven parent molecules and in total 18 isomers, with the H and D pair attached at different positions (see Figure 3). For each parent molecule, the mean spectrum averaged over all the isomers is given in Figures 10a–g. The overall mean spectrum averaged over seven parent molecules is shown in Figure 10h. It is apparent that, upon ionization, the C–H and C–D stretches are substantially depressed, while the C–C stretches at $\sim 6\text{--}9 \mu\text{m}$ are appreciably enhanced. The wavelengths and intensities of the C–H and C–D stretches are tabulated in Table 3 and shown in Figure 11. With $\langle \lambda_{\text{peak}} \rangle \approx 4.76 \pm 0.05 \mu\text{m}$ and $\langle A_{4.65} \rangle \approx 1.64 \pm 0.75 \text{ km mol}^{-1}$, the aliphatic C–D stretches of “superdeuterated” PAH cations peak at significantly longer wavelengths and are ~ 10 times weaker than that of neutrals.

3.3. PAHs with Both Aromatic and Aliphatic C–D Bonds

Considering that the aliphatic C–D bands at $\sim 4.6\text{--}4.8\ \mu\text{m}$ are always seen in emission together with the aromatic C–D bands at $\sim 4.4\ \mu\text{m}$ (Peeters et al. 2004; Onaka et al. 2014, 2022; Doney et al. 2016), we also calculate the vibrational spectra of PAHs with both aliphatic and aromatic C–D bonds, with pyrene as an illustrative example. We consider two kinds of aliphatic C–D units, with the aliphatic D atom either in a methyl group (hereafter PyreD_CH₂D, see Figure 4) or in a “superdeuterated” pair (i.e., one D atom and one H atom share an C atom; hereafter PyreD_HD, see Figure 5). We consider 23 isomers for PyreD_CH₂D, with the deuterated-methyl group attached at position 1, 2 or 4, and the other D atom bonding with one of the remaining edge C atoms in pyrene. For PyreD_HD, we consider 24 isomers, with the H+H pair and the H+D pair attached at positions 1 and 2, 2 and 3, or 4 and 5, while the other D atom, again, bonding with one of the remaining edge C atoms in the rings.

By categorizing the isomers according to the positions of the aliphatic D atom, we show in Figure 12 the spectra of the isomers in each category. We also obtain the mean spectrum by averaging over all the isomers and show in Figure 14. The aliphatic and aromatic C–D stretches respectively at $2170\ \text{cm}^{-1}$ (i.e., $4.61\ \mu\text{m}$) and $2250\ \text{cm}^{-1}$ (i.e., $4.44\ \mu\text{m}$) are clearly seen in the spectra of isomers as well as in the mean spectrum, with the aliphatic C–D stretch being appreciably more intense than the aromatic C–D stretch. It is interesting to note that the spectra of different isomers are quite similar (see Figures 12, 14), implying that the positions of the D atoms do not significantly affect the spectra.

The wavelengths and intensities of the C–H and C–D stretches of PyreD_CH₂D and PyreD_HD are respectively tabulated in Tables 4, 5, and the intensities are shown in Figures 13, 15. With $\langle\lambda_{\text{peak}}\rangle \approx 4.41\ \mu\text{m}$ and $\langle A_{4.65}\rangle \approx 7.9\ \text{km mol}^{-1}$, the wavelengths and intensities of the aromatic C–D stretch in PyreD_CH₂D are essentially consistent with that of PyreD_HD. This is not surprising because, according to the Born-Oppenheimer approximation, the presence of an D-substituted methyl sidegroup or a pair of H and D atoms sharing one C atom would not affect the aromatic C–D stretches. On the other hand, the intensities of the aliphatic C–D stretches of PyreD_CH₂D ($\langle A_{4.65}\rangle \approx 12.4\ \text{km mol}^{-1}$) differ appreciably from that of PyreD_HD ($\langle A_{4.65}\rangle \approx 19.5\ \text{km mol}^{-1}$). This is understandable since they arise from different types of aliphatic C–D units.

3.4. Aliphatic C–D Band Intensities

In Figures 16–20, we show $A_{4.65}/A_{3.3}$ —the band-intensity ratio of the 4.65 μm aliphatic C–D stretch to that of the 3.3 μm aromatic C–H stretch—calculated for each set of our target molecules. Generally speaking, $A_{4.65}/A_{3.3}$ does not vary much from one molecule to another in each set. We obtain $\langle A_{4.65}/A_{3.3} \rangle \approx 0.90 \pm 0.07$ for PAHs attached with a D-substituted methyl sidegroup (PAH_CH₂D), and $\langle A_{4.65}/A_{3.3} \rangle \approx 1.10 \pm 0.32$ for “superdeuterated” PAHs (PAH_HD) in which an extra D atom shares an C atom with an H atom. For pyrenes attached with a D-substituted methyl sidegroup (PyreD_CH₂D), we obtain $\langle A_{4.65}/A_{3.3} \rangle \approx 0.85$ with a standard deviation of ~ 0.12 ; for “superdeuterated” pyrenes (PyreD_HD), we obtain $\langle A_{4.65}/A_{3.3} \rangle \approx 1.31$ with a standard deviation of ~ 0.17 .

In Table 6 we summarize the *mean* band strengths of the aliphatic C–D and aromatic C–H stretches, obtained by averaging over all the species considered here. The recommended band intensities are $\langle A_{4.65} \rangle \approx 15.3 \pm 3.3 \text{ km mol}^{-1}$, $\langle A_{3.3} \rangle \approx 14.8 \pm 0.33 \text{ km mol}^{-1}$, and $\langle A_{4.65}/A_{3.3} \rangle \approx 1.04 \pm 0.21$ for deuterated neutral PAHs, and $\langle A_{4.65} \rangle \approx 1.64 \pm 0.75 \text{ km mol}^{-1}$, $\langle A_{3.3} \rangle \approx 2.14^{+3.08}_{-2.14} \text{ km mol}^{-1}$, and $\langle A_{4.65}/A_{3.3} \rangle \approx 1.67 \pm 1.00$ for deuterated PAH cations.² Since the intensities for the C–H or C–D stretches are significantly depressed for PAH cations, when estimating the D enrichment from astronomical observations, we recommend to adopt $A_{4.65}/A_{3.3} \approx 1.04 \pm 0.21$, the band-intensity ratio of deuterated neutral PAHs.

4. Astrophysical Applications

4.1. Aliphatic C–D Bands: Astronomical Observations

Observational efforts have been made with the *Short Wavelength Spectrometer* (SWS) on board the *Infrared Space Observatory* (ISO) and the *Infrared Camera* (IRC) on board AKARI to search for signals of deuterated PAHs through their vibrational C–D bands (Verstraete et al. 1996; Peeters et al. 2004; Onaka et al. 2014, 2022; Doney et al. 2016). So far, the detection of the aliphatic C–D bands has been reported in eight sources (Peeters et al. 2004, Onaka et al. 2014, Doney et al. 2016). We compile all the available observational data for the 3.3 μm aromatic C–H stretch, the 3.4 μm aliphatic C–H stretch, the 4.4 μm aromatic C–D

²The large scatter in $\langle A_{3.3} \rangle$ for PAH cations mainly arises from the large $A_{3.3}$ intensity of Benz_HD+ (see Table 3), which is substantially larger than that of the other molecules. If we exclude Benz_HD+, we obtain $\langle A_{3.3} \rangle \approx 1.00 \pm 0.59 \text{ km mol}^{-1}$ and $\langle A_{4.65}/A_{3.3} \rangle \approx 1.92 \pm 0.94$. However, this does not affect the degree of deuteration of PAHs derived below in §4.2 since the C–D and C–H stretches are dominated by neutral PAHs

stretch, and the “4.65” μm aliphatic C–D stretch.³ The observational emission intensities of these stretches ($I_{3.3}$, $I_{3.4}$, $I_{4.4}$, and $I_{4.65}$) and their ratios with respect to the 3.3 μm aromatic C–H stretch, $(I_{4.65}/I_{3.3})_{\text{obs}}$, $(I_{4.4}/I_{3.3})_{\text{obs}}$ and $(I_{3.4}/I_{3.3})_{\text{obs}}$ are summarized in Table 7.

We explore whether these stretching bands are somewhat related to each other. Figure 21a compares the observed emission intensities of the aliphatic C–D stretch ($I_{4.65}$) with that of the aromatic C–D stretch ($I_{4.4}$). No correlation is found between $I_{4.65}$ and $I_{4.4}$. To eliminate their common correlation with the starlight radiation field (i.e., the observed emission intensities of all these bands are proportional to the starlight intensity), we normalize $I_{4.65}$ and $I_{4.4}$ by $I_{3.3}$ and then compare $I_{4.65}/I_{3.3}$ with $I_{4.4}/I_{3.3}$. As demonstrated in Figure 21b, $I_{4.65}/I_{3.3}$ and $I_{4.4}/I_{3.3}$ are not correlated. This indicates that the deuteration of the aliphatic C atoms may not occur together with the deuteration of the aromatic C atoms (i.e., the aliphatic and aromatic C atoms get deuterated independently). Also, to examine the degree of deuteration of the aliphatic C atoms and that of the aromatic C atoms, we compare $I_{4.65}/I_{3.4}$ with $I_{4.4}/I_{3.3}$ and find no correlation either (see Figure 21c). This also implies that the deuterations of the aliphatic and aromatic C atoms occur independently. Finally, we compare $I_{4.65}/I_{4.4}$ with $I_{3.4}/I_{3.3}$. This is to investigate if the aliphaticity of the C–D bond is related to that of the C–H bond. As shown in Figure 21d, they do not correlate.

4.2. Deuterium Depletion onto PAHs

We now evaluate from the observed emission intensities of the 4.65 μm aliphatic C–D stretch the number of D atoms (relative to H) that could have been locked up in the aliphatic C–D units of PAHs. For a PAH molecule containing N_{H} aromatic H atoms, and N_{D} aliphatic D atoms, we define the degree of deuteration of the molecule as $f_{\text{aliCD}} \equiv N_{\text{D}}/(N_{\text{H}} + N_{\text{D}})$, the fraction of the total (H and D) atoms in the form of D. The *observed* ratio of the power emitted from the 4.65 μm aliphatic C–D band to that from the 3.3 μm aromatic C–H band is related to the degree of deuteration through

$$\left(\frac{I_{4.65}}{I_{3.3}}\right)_{\text{obs}} \approx \left(\frac{A_{4.65}}{A_{3.3}}\right) \times \left(\frac{N_{\text{C-D}}}{N_{\text{C-H}}}\right) \times \left(\frac{B_{4.65}}{B_{3.3}}\right), \quad (1)$$

where $N_{\text{C-H}}$ and $N_{\text{C-D}}$ are respectively the number of C–H and C–D bonds in a deuterated PAH molecule, $B_{\lambda}(T)$ is the Planck function at wavelength λ and temperature T , and $A_{3.3}$ and $A_{4.65}$ are the intrinsic band strengths of the aromatic C–H and aliphatic C–D stretches

³The aliphatic C–D stretch of PAHs, consisting of asymmetric and symmetric modes, actually spans a range of wavelengths, from $\sim 4.6 \mu\text{m}$ to $\sim 4.8 \mu\text{m}$. In this work, by “4.65 μm ” we actually mean the aliphatic C–D stretch over the wavelength range of $\sim 4.6\text{--}4.8 \mu\text{m}$.

(on a per C–H or C–D bond basis). Since the observed C–H and C–D stretching emission bands arise predominantly from neutral PAHs, we will adopt $A_{4.65}/A_{3.3} \approx 1.04 \pm 0.21$ calculated for neutral PAHs containing aliphatic C–D units (see §3.4 and Table 6).

Considering the relatively small abundance of D atoms in space, it is unlikely that an aliphatic C atom would be doubly deuterated (i.e., two D atoms share one C atom). Therefore, it is reasonable to assume $N_{\text{C–D}} = N_{\text{D}}$ and $N_{\text{C–H}} = N_{\text{H}}$. The degree of deuteration of the molecule becomes

$$f_{\text{aliCD}} \approx \left\{ 1 + \left(\frac{I_{3.3}}{I_{4.65}} \right)_{\text{obs}} \times \left(\frac{A_{4.65}}{A_{3.3}} \right) \times \left(\frac{B_{4.65}}{B_{3.3}} \right) \right\}^{-1}. \quad (2)$$

The 3.3 μm C–H stretch and 4.65 μm C–D stretch are most effectively emitted respectively by PAHs of vibrational temperatures of ~ 730 K and ~ 520 K (see Footnote No. 10 in Yang et al. 2020), stochastically heated by individual UV photons (Draine & Li 2001). For $520 \lesssim T \lesssim 730$ K, we obtain $B_{3.3}/B_{4.65} \approx 0.72 \pm 0.14$. By relaxing the temperature range to $400 \lesssim T \lesssim 900$ K, we obtain $B_{3.3}/B_{4.65} \approx 0.78 \pm 0.32$. Even if we extend the temperature range to $300 \lesssim T \lesssim 1000$ K, a similar ratio of $B_{3.3}/B_{4.65} \approx 0.78 \pm 0.44$ is still obtained. In the following, we will adopt $B_{3.3}/B_{4.65} \approx 0.78 \pm 0.32$ that is suitable for $400 \lesssim T \lesssim 900$ K.

With $B_{3.3}/B_{4.65} \approx 0.78 \pm 0.32$ and $A_{4.65}/A_{3.3} \approx 1.04 \pm 0.21$ (see §3.4), for each of the eight sources we obtain f_{aliCD} from $(I_{4.65}/I_{3.3})_{\text{obs}}$. These sources also exhibit an aromatic C–D stretch at $\sim 4.4 \mu\text{m}$ as well as an aliphatic C–H stretch at $3.4 \mu\text{m}$. Following Yang et al. (2020), for each source we derive f_{aroCD} , the deuteration degree of PAHs based on the aromatic C–D stretch. Similarly, following Yang et al. (2013), for each source we also derive f_{aliCH} , the aliphatic fraction of PAHs based on the aliphatic C–H stretch. The results are tabulated in Table 7.

It is gratifying that in some sources (e.g., NGC 3603, IRAS 12073, M17b) f_{aliCD} can be as much as $\sim 20\%$, implying that PAHs could be a plausible sink of the missing D atoms. In the ISM, PAHs require a total C/H abundance of $[\text{C}/\text{H}]_{\text{PAH}} \approx 60$ ppm (Li & Draine 2001), where $[\text{C}/\text{H}]_{\text{PAH}}$ refers to the amount of C locked up in PAHs (relative to the total H in the ISM). For small PAHs like coronene, the ratio of the number of C atoms to the number of H atoms is $N_{\text{C}}/N_{\text{H}} \approx 2$. Therefore, PAHs may contain an amount of ~ 30 ppm of H (relative to the total H in the ISM). A combination of f_{aliCD} and f_{aroCD} indicates that in some sources up to $\sim 28\%$ of the H atoms in PAHs could be deuterated (see Table 7), i.e., $[\text{D}/\text{H}]_{\text{PAH}} \approx 8.4$ ppm – the amount of D locked up in PAHs (relative to the total H in the ISM). This exceeds the median of the missing D/H (~ 7 ppm; see §1). We note that aliphatic C–D is often created from the deuteration of methyl-group or superdeuteration. This naturally accompanies with at least one aliphatic C–H bond. Therefore, one would expect a higher f_{aliCH} than f_{aliCD} . Indeed, Table 7 shows that in some sources f_{aliCH} is twice as much as f_{aliCD} .

Finally, we should also note that the above estimation of ≈ 8.4 ppm of D depleted in PAHs (relative to the total H in the ISM) is rather generous. This is based on the assumption that both small ($N_C \lesssim 40$) and large PAHs ($N_C \gtrsim 100$) are deuterated. For large PAHs, deuteration may occur in D-enriched ice mantles (see §4.3). Even if they are deuterated, due to their large heat capacities, large PAHs are not excited sufficiently to temperatures high enough to emit at the C–H and C–D stretching bands.

In addition to large PAHs, hydrogenated amorphous carbon (HAC) solids could also deplete some of the D atoms missing from the gas phase. Furton et al. (1999) found that the interstellar $3.4 \mu\text{m}$ aliphatic C–H *absorption* band is most consistent with ~ 80 ppm of C (relative to the total H in the ISM) with an H/C ratio of ~ 0.5 . Compared with PAHs, HAC would provide a larger number of potential sites for D-depletion. It would be interesting to see if the lines of sight exhibiting strong $3.4 \mu\text{m}$ aliphatic C–H absorption also show detectable aliphatic C–D absorption at $\sim 4.65 \mu\text{m}$.

In the local diffuse ISM, the optical depth of the $3.4 \mu\text{m}$ aliphatic C–H *absorption* relative to the visual extinction (A_V) is $\Delta\tau_{3.4 \mu\text{m}}/A_V \approx 1/274$ (Sandford et al. 1991, Pendleton et al. 1994; see Gao et al. 2010 for a summary). Toward the Galactic center, with $\Delta\tau_{3.4 \mu\text{m}}/A_V \approx 1/146$ (McFadzean et al. 1989, Pendleton et al. 1994; also see Gao et al. 2010 for a summary), the $3.4 \mu\text{m}$ absorption band is stronger (on a per magnitude of visual extinction basis) by a factor of ~ 1.9 . If we take the band-intensity ratio of the $4.65 \mu\text{m}$ aliphatic C–D to the $3.4 \mu\text{m}$ aliphatic C–H to be $A_{4.65}/A_{3.4} \approx 0.38$ as measured for deuterated quenched carbonaceous composite materials (Mori et al. 2022), and assume that HAC contains ~ 40 ppm of H and ~ 7 ppm of D (relative to the total H in the ISM), we expect the optical depth of the $4.65 \mu\text{m}$ aliphatic C–D absorption relative to the visual extinction to be $\Delta\tau_{4.65 \mu\text{m}}/A_V \approx 1/4150$ for the local ISM and $\Delta\tau_{4.65 \mu\text{m}}/A_V \approx 1/2200$ for the Galactic center. Such a weak band is beyond the detection capability of ISO. JWST’s unprecedented sensitivity will provide a unique opportunity to detect or place an upper limit on the $4.65 \mu\text{m}$ aliphatic C–D *absorption* band in heavily obscured lines of sight.

4.3. Possible Routes for Aliphatically Deuterating PAHs

A significant fraction of the UV radiation emitted by massive stars impinges on the molecular gas associated with star formation. This results in a PDR bounded on one side by an ionization front, and on the other side by cold molecular gas which has not yet been appreciably affected by UV radiation.

As schematically illustrated in Figure 22, it is natural to expect that interstellar PAHs

are deuterated in such regions. Lets take the Orion Bar as an example. The regions close to the ionization front are rich in UV photons and deuteration could occur during photodissociation events. Upon absorption of an energetic photon, one or more peripheral H atoms could be stripped off and replaced by D atoms. Due to the zero-point energy difference, C–D bonds are more stable than C–H bonds and therefore PAHs of intermediate size are expected to become deuterium enriched and obtain aromatic C–D units. In these regions one expects to see the $4.4\ \mu\text{m}$ emission band arising from aromatic C–D stretch.

When moving away from the ionization front, the regions intermediate between the ionization front and the dissociation front, are rich in H and D atoms. PAHs could be superhydrogenated (i.e., two H atoms share one C atom) and even superdeuterated (i.e., one D atom and one H atom share one C atom). In these regions one expects to see the aliphatic C–D stretching emission at $\sim 4.6\text{--}4.8\ \mu\text{m}$ as well as the aliphatic C–H stretching emission at $3.4\ \mu\text{m}$ (see Figure 22 for illustration).

Another way to deuterate PAHs and generate aliphatic C–D bonds is through the addition of a D-substituted methyl group. This could occur in dense clouds where PAHs and simple molecules (e.g., CH_4) are frozen into the ice mantles coated on dust grains. In D-enriched ices, exposed to UV irradiation, PAHs could attain a D-substituted methyl group through chemical reactions with deuterated methane (see Figure 23 for a schematic illustration). PAHs could also become deuterated in D-enriched ices by exchanging H atoms with D atoms. This H/D exchange would be enhanced for oxidized PAHs. Furthermore, UV-stimulated addition of D atoms at aromatic edge sites could yield aliphatic C–D bonds. Sandford et al. (2000) have experimentally demonstrated that, when exposed to UV radiation, PAHs in D-enriched ices could be oxidized and easily deuterated.

As deuterated PAHs made in UV-irradiated ices are likely also oxidized, we also compute the vibrational spectra of deuterated, oxidized PAHs, taking coronene as an example. We consider two coronene derivatives, with D-atom exchange at oxidized edge sites or at aromatic edge sites. The structures of these two molecules are also shown in Figure 2. We show in Figure 24 their vibrational spectra, together with two “superdeuterated” species. The aliphatic and aromatic C–D stretches as well as the O–D stretch are clearly seen. We note that in Coro_O2D (in which two D atoms are attached to one C atom) the aliphatic C–D stretch is significantly depressed.

5. Summary

We have explored whether interstellar PAHs could be a major reservoir of D to account for its depletion from the gas phase, focusing on the aliphatic C–D units of PAHs. The major results are as follows:

1. We have employed the hybrid DFT method B3LYP in conjunction with the 6-311+G** basis set to calculate the vibrational spectra of deuterated PAHs with aliphatic C–D units, including “superdeuterated” PAHs in which one D and one H share an C atom and PAHs attached with an D-substituted methyl group.
2. For all these aliphatically deuterated species and their isomers, we have derived from the computed spectra the intrinsic band strengths of the 4.65 μm aliphatic C–D stretch ($A_{4.65}$), and the 3.3 μm aromatic C–H stretch ($A_{3.3}$). Both the C–H and C–D stretches predominantly arise from neutral PAHs. By averaging over all these molecules, we have determined the mean band strengths to be $\langle A_{4.65} \rangle \approx 15.3 \pm 3.3 \text{ km mol}^{-1}$, $\langle A_{3.3} \rangle \approx 14.8 \pm 0.33 \text{ km mol}^{-1}$, and $\langle A_{4.65}/A_{3.3} \rangle \approx 1.04 \pm 0.21$.
3. We have compiled all the observational data from ISO/SWS and AKARI/IRC and derived $(I_{4.4}/I_{3.3})_{\text{obs}}$, the ratio of the power emitted from the aliphatic C–D band at 4.6–4.8 μm ($I_{4.65}$) to that from the aromatic C–H band at 3.3 μm ($I_{3.3}$). By comparing the computationally-derived mean ratio of $\langle A_{4.65}/A_{3.3} \rangle \approx 1.04$ for aliphatically deuterated PAHs, it is found the degree of deuteration of some sources could be as high as $\sim 20\%$. Combined with PAHs containing aromatic C–D units, the amount of D/H tied up in deuterated PAHs could exceed that missing from the gas phase, therefore consistent with the predictions from the BBN and GCE models and the gas-phase D/H of the local ISM.
4. It is not clear how the high deuteration of PAHs required to account for the missing D is achieved. We have suggested that the deuteration of PAHs with aromatic C–D units may mainly occur in UV-rich regions, while the deuteration of PAHs with aliphatic C–D units may mainly occur in benign regions rich in H and D atoms or in dense clouds.

We thank B.T. Draine, A.N. Witt and the anonymous referee for valuable suggestions. XJY is supported in part by NSFC 12122302 and 11873041. AL is supported in part by NASA grants 80NSSC19K0572 and 80NSSC19K0701.

REFERENCES

- Allamandola, L.J., Tielens, A.G.G.M., & Barker, J.R. 1985, ApJ, 290, L25
- Buragohain, M., Pathak, A., Sarre, P., Onaka, T., & Sakon, I. 2015, MNRAS, 454, 193
- Buragohain, M., Pathak, A., Sarre, P., Onaka, T., & Sakon, I. 2016, Planet. Space Sci., 133, 97
- Buragohain, M., Pathak, A., Sakon, I., & Onaka, T. 2020, ApJ, 892, 11
- Doney, K. D., Candian, A., Mori, T., Onaka, T., & Tielens, A. G. G. M. 2016, A&A, 586, 65
- Draine, B. T. 2006, in ASP Conf. Ser. 348, Astrophysics in the Far Ultraviolet: Five Years of Discovery with FUSE, ed. G. Sonneborn, H. Moos, & B. -G. Andersson (San Francisco, CA: ASP), 58
- Draine, B.T., & Li, A. 2001, ApJ, 551, 807
- Frisch, M. J., Trucks, G. W., Schlegel, H. B., et al. 2016, Gaussian 16, Revision C.01, Gaussian, Inc., Wallingford CT
- Furton, D. G., Laiho, J. W., & Witt, A. N. 1999, ApJ, 526, 752
- Gao, J., Jiang, B.W., & Li, A. 2010, EPS, 62, 63
- Hudgins, D. M., Bauschlicher, C. W., Jr., & Sandford, S. A. 2004, ApJ, 614, 770
- Li, A., & Draine, B.T. 2001, ApJ, 554, 778
- McFadzean, A. D., Whittet, D.C.B., Bode, M.F., Adamson, A.J., & Longmore, A.J. 1989, MNRAS, 241, 873
- Mori, T., Onaka, T., Sakon, I., et al. 2022 ApJ, 933, 35
- Onaka, T., Mori, T. I., Sakon, I., et al. 2014, ApJ, 780, 114
- Onaka, T., Sakon, I., & Shimonishi, T., 2022, ApJ, 941, 190
- Pendleton, Y.J., Sandford, S.A., Allamandola, L.J., Tielens, A.G.G.M., & Sellgren, K. 1994, ApJ, 437, 683
- Peeters, E., Allamandola, L. J., Bauschlicher, C. W., Jr., et al. 2004, ApJ, 604, 252

- Sandford, S.A., Allamandola, L.J., Tielens, A.G.G.M., Sellgren, K., Tapia, M., & Pendleton, Y.J. 1991, *ApJ*, 371, 607
- Sandford, S. A., Bernstein, M. P., Allamandola, L. J., Gillette, J. S., & Zare, R. N. 2000, *ApJ*, 538, 691
- Tielens, A. G. G. M. 1997, *Astrophysical Implications of the Laboratory Study of Presolar Materials*, ed T. H. Bernatowicz & E. K. Zinner (New York: AIP) 523
- Verstraete, L., Puget, J. L., Falgarone, E., et al. 1996, *A&A*, 315, L337
- Yang, X. J., Glaser, R., Li, A., & Zhong, J. X. 2013, *ApJ*, 776, 110
- Yang, X. J., Glaser, R., Li, A., & Zhong, J. X. 2017, *New Astron. Rev.*, 77, 1
- Yang, X. J., Li, A., & Glaser, R. 2020, *ApJS*, 251, 12
- Yang, X. J., Li, A., He, C. Y., & Glaser, R. 2021, *ApJS*, 255, 23

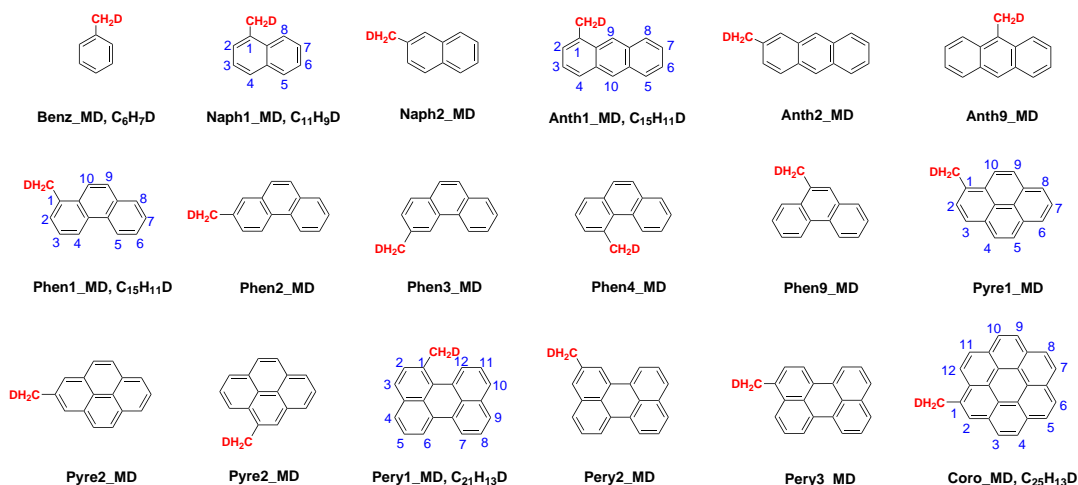


Fig. 1.— Structures of methyl-deuterated PAHs. We refer to a methyl-deuterated species by the abbreviation of the first four letters of the name of its parent molecule followed by the position where the methyl group is attached (e.g., Anth2 refers to anthracene with the deuterated methyl attached at position 2). Since there are three H atoms in methyl and any of them could be deuterated, therefore all three possibilities are taken into account.

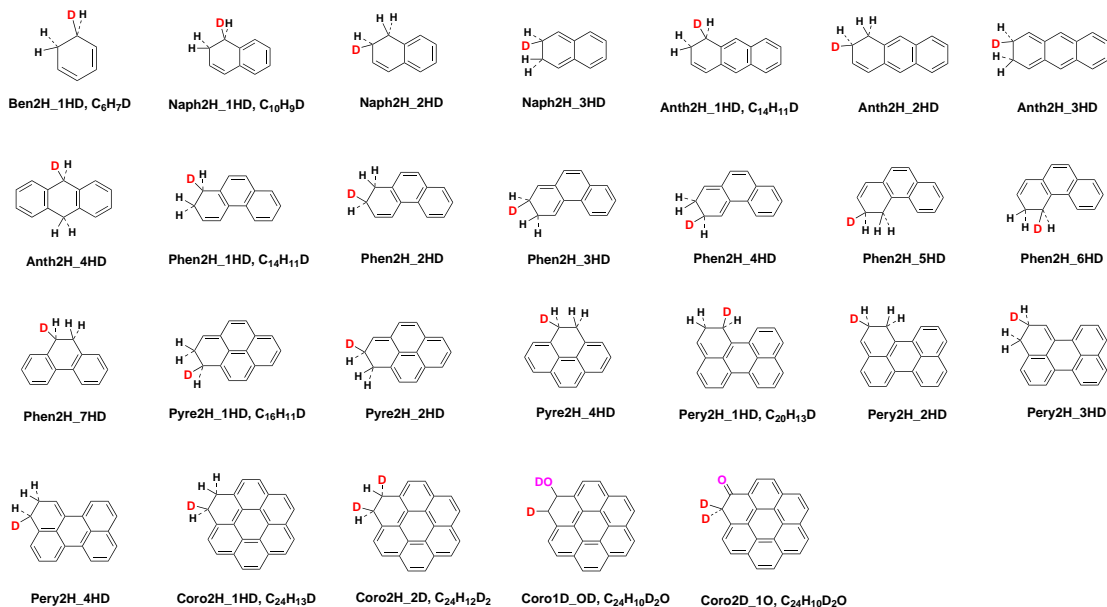


Fig. 2.— Structures of “superdeuterated” PAHs in which one D and one H atom share an C atom. Since H is much more abundant than D in space, if a PAH molecule is “superdeuterated”, it is very likely that it will also be superhydrogenated. Also shown are doubly “superdeuterated” coronene (with two pairs of H and D atoms), and deuterated, oxidized coronenes (see §4.3).

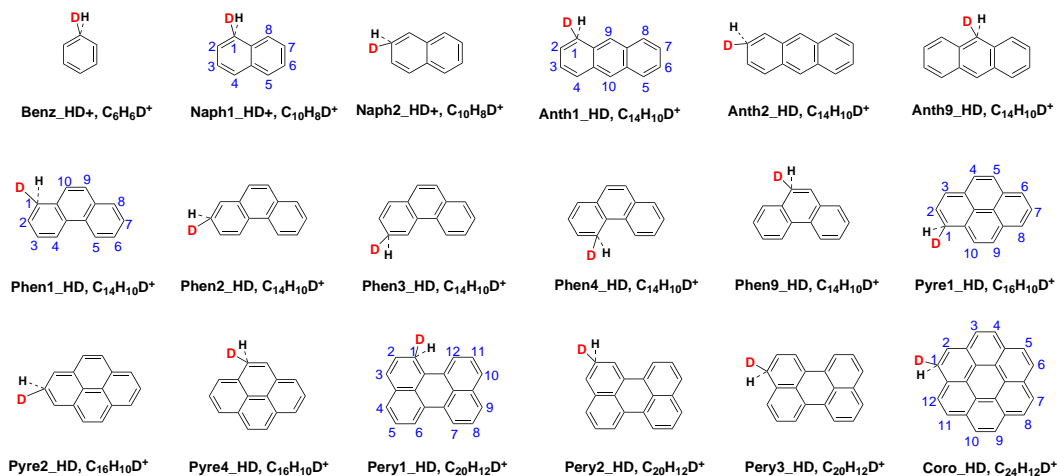


Fig. 3.— Structures of “superdeuterated” PAH cations.

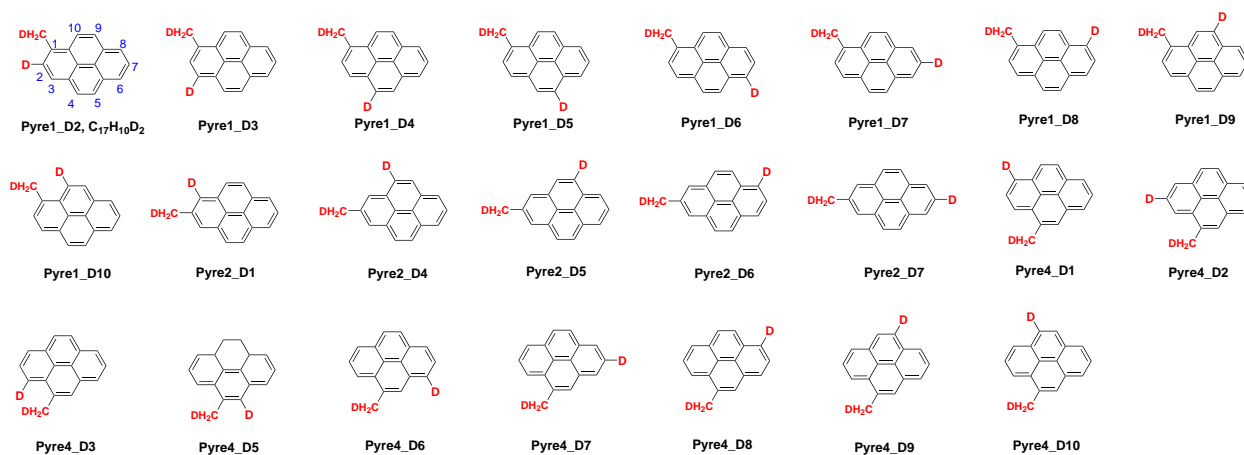


Fig. 4.— Structures of 23 isomers of deuterated pyrenes containing a methyl-deuterated sidegroup as well as a periph al D atom. These molecules have both aliphatic and aromatic C–D bonds.

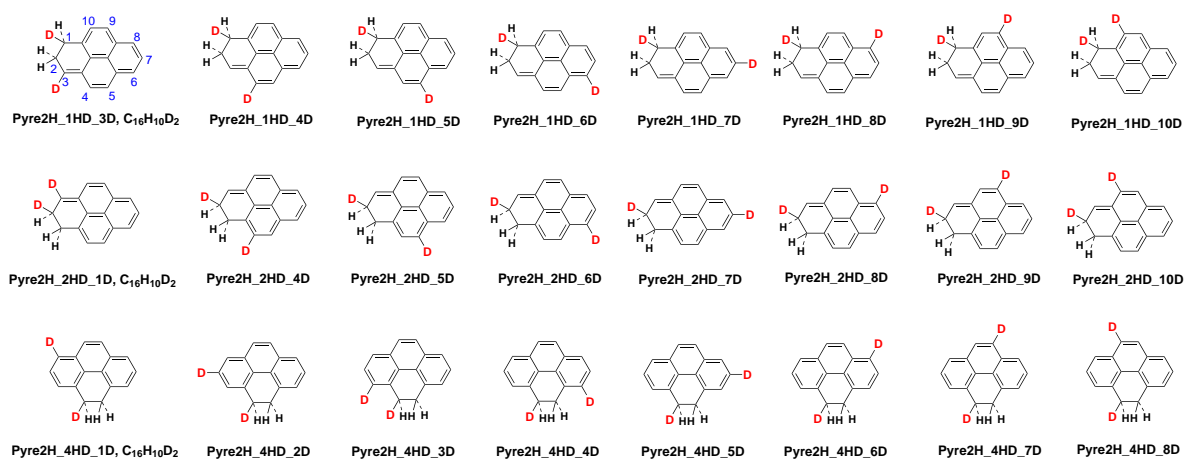


Fig. 5.— Structures of 24 isomers of “superdeuterated” pyrenes containing an H+H pair, an H+D pair, as well as a periphial D atom. Similar to that in Figure 4, these molecules also have both aliphatic and aromatic C–D bonds.

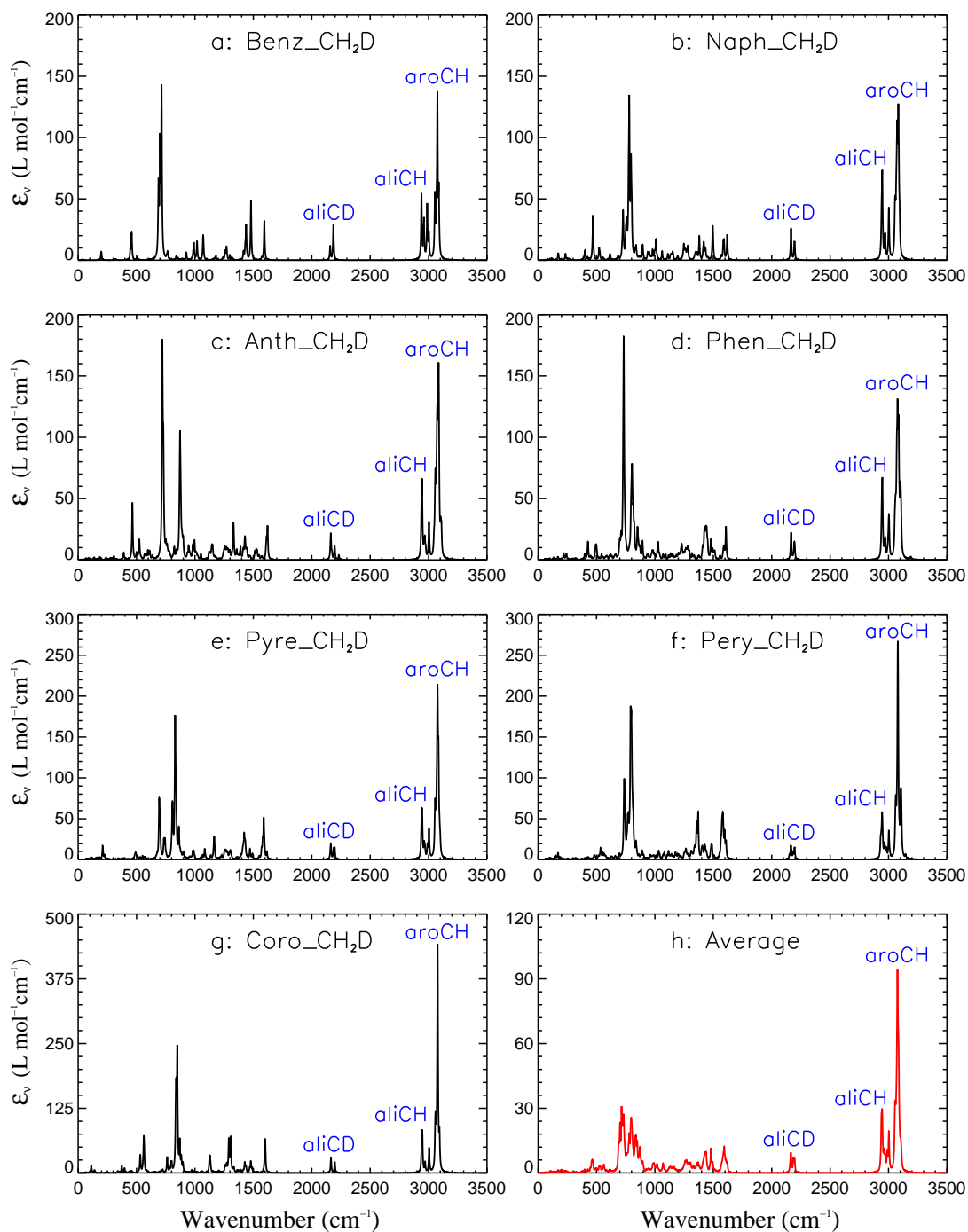


Fig. 6.— DFT-computed vibrational spectra of methyl-deuterated PAHs (see Figure 1), obtained by averaging over all the isomers of each parent molecule. Also shown is the overall mean spectrum obtained by averaging over the mean spectra of all seven parent molecules (normalized by N_C). The aliphatic C–D, aliphatic C–H, and aromatic C–H stretches are labelled respectively by “aliCD”, “aliCH” and “aroCH”.

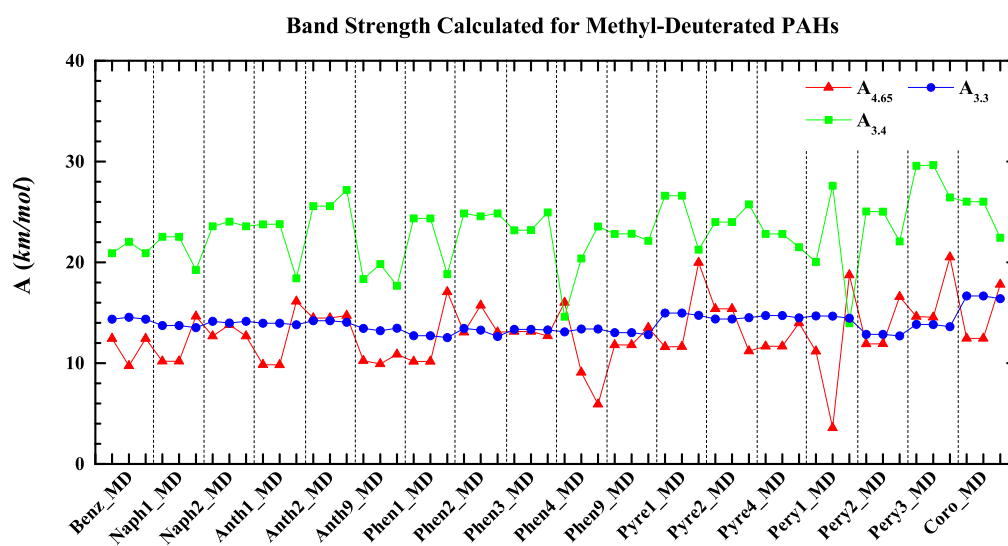


Fig. 7.— Band strengths of the $4.65\ \mu\text{m}$ aliphatic C–D stretches ($A_{4.65}$; red), the $3.4\ \mu\text{m}$ aliphatic C–H stretches ($A_{3.4}$; green), and the $3.3\ \mu\text{m}$ aromatic C–H stretches ($A_{3.3}$; blue) computed at level B3LYP/6-311+G** for methyl-deuterated PAHs.

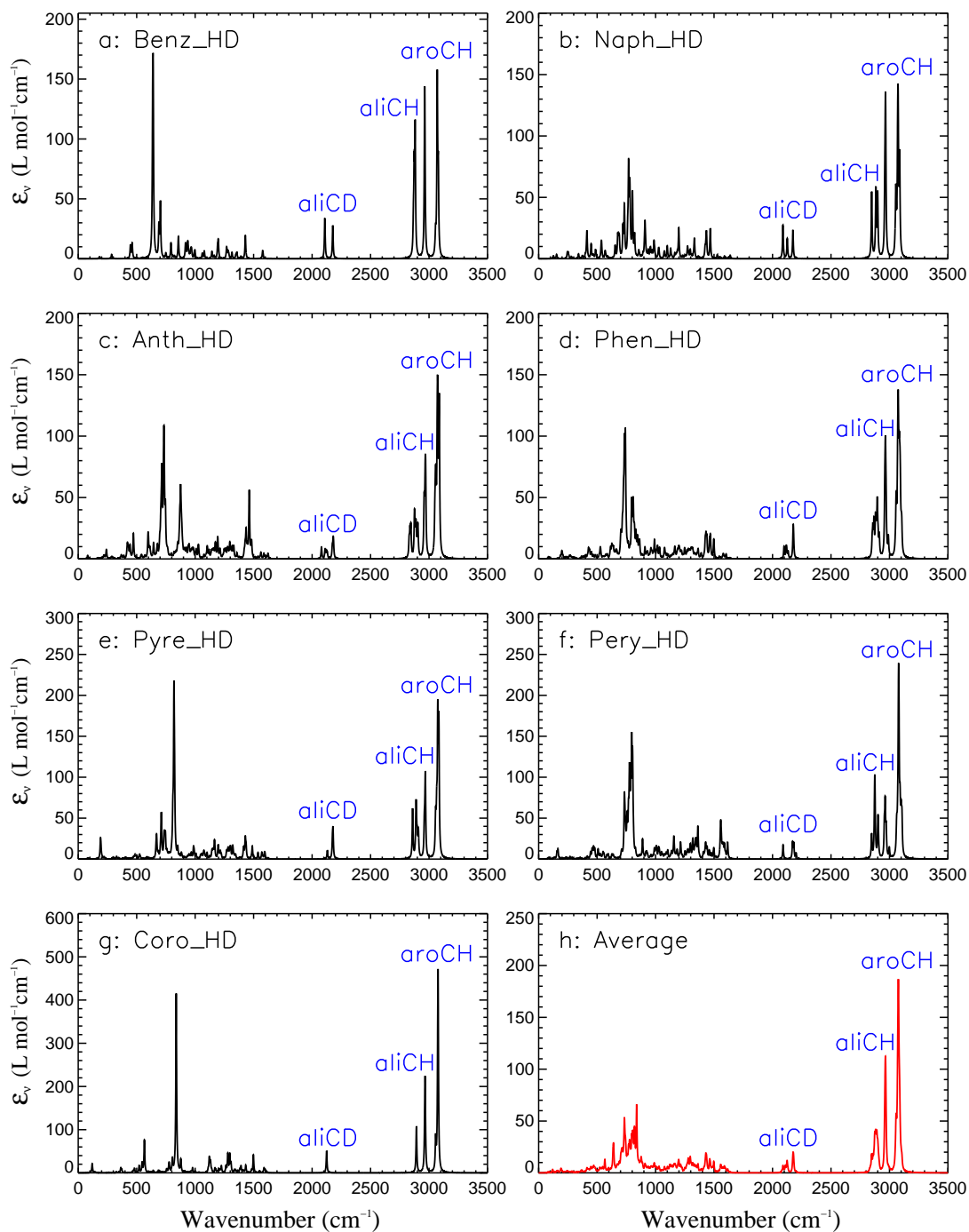


Fig. 8.— Same as Figure 6 but for “superdeuterated” PAHs in which one H atom and one D atom share an C atom (see Figure 2).

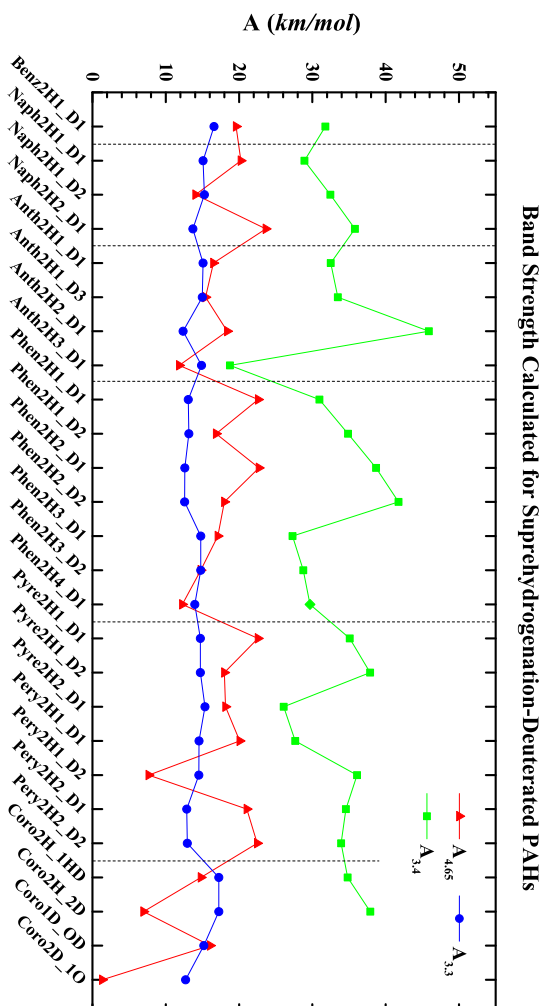


Fig. 9. — Same as Figure 7 but for “superdeuterated” PAHs.

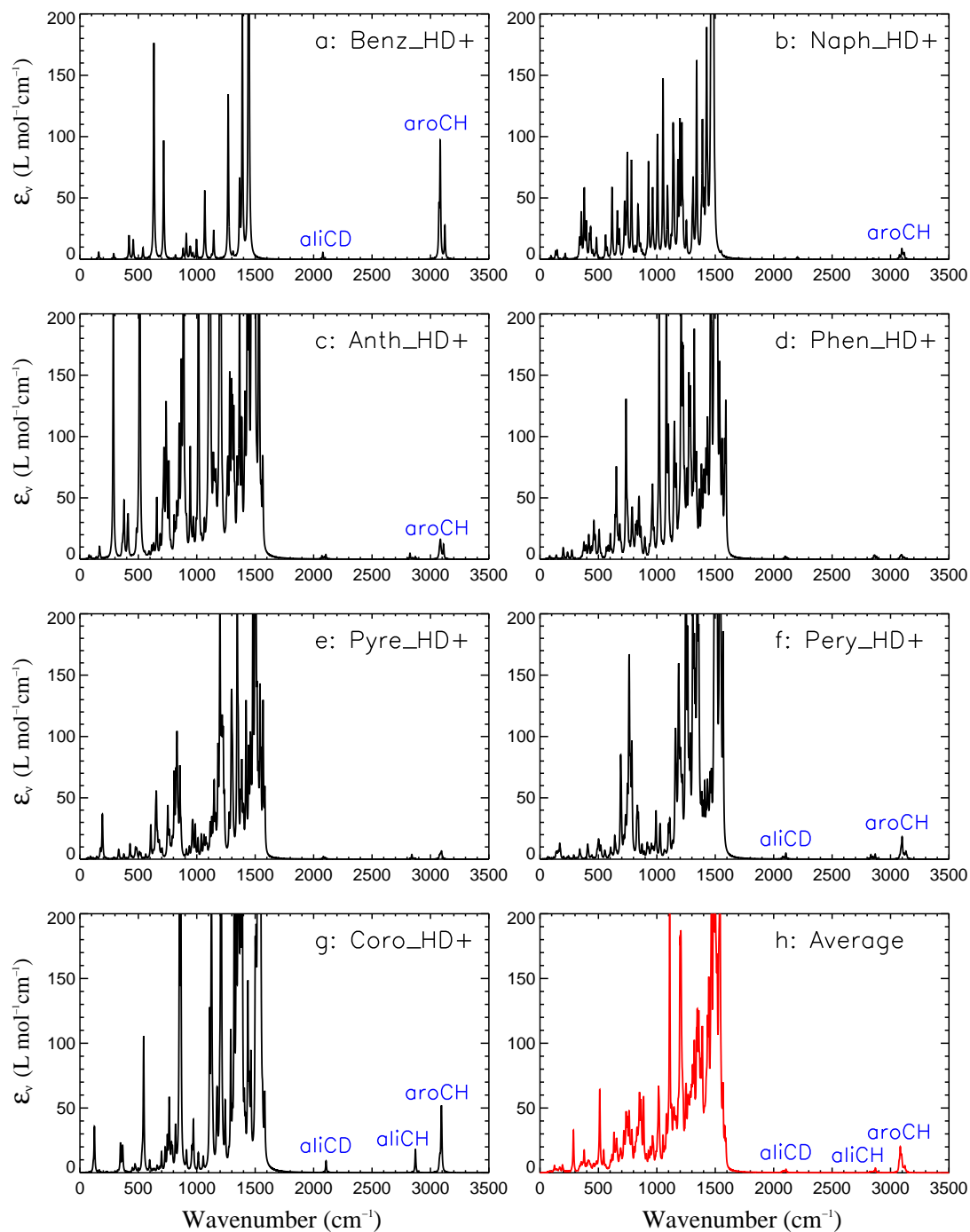


Fig. 10.— Same as Figure 6 but for “superdeuterated” PAH cations (see Figure 3).

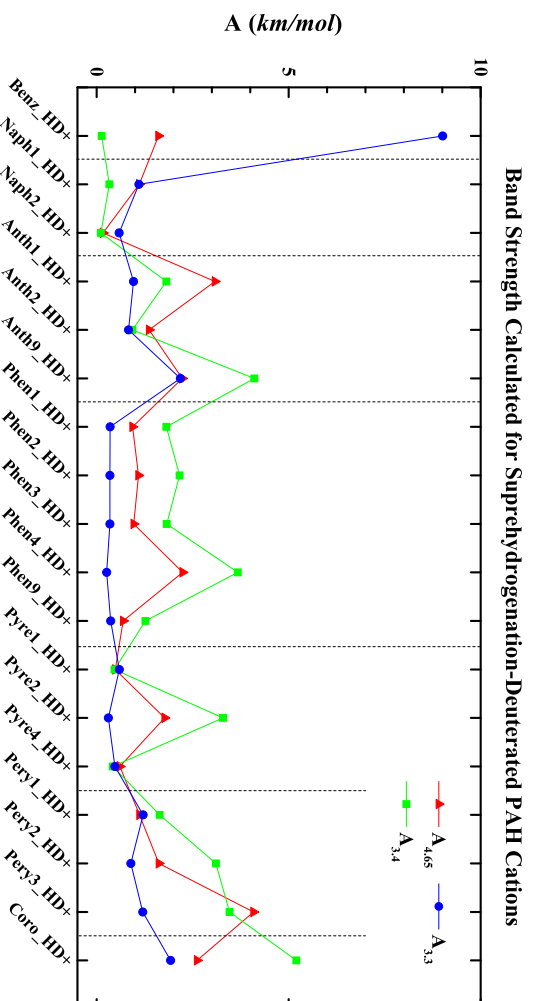


Fig. 11.— Same as Figure 7 but for “superdeuterated” PAH cations.

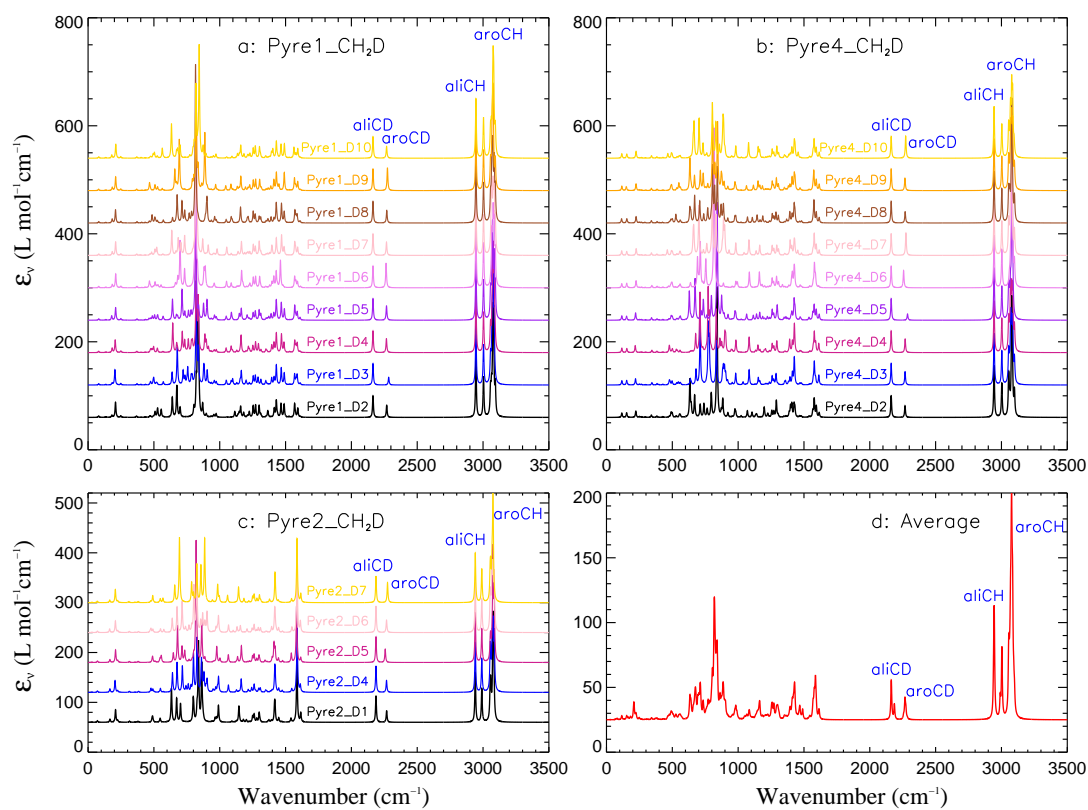


Fig. 12.— Same as Figure 6 but for pyrenes containing a methyl-deuterated sidegroup as well as a peripheral D atom (see Figure 4).

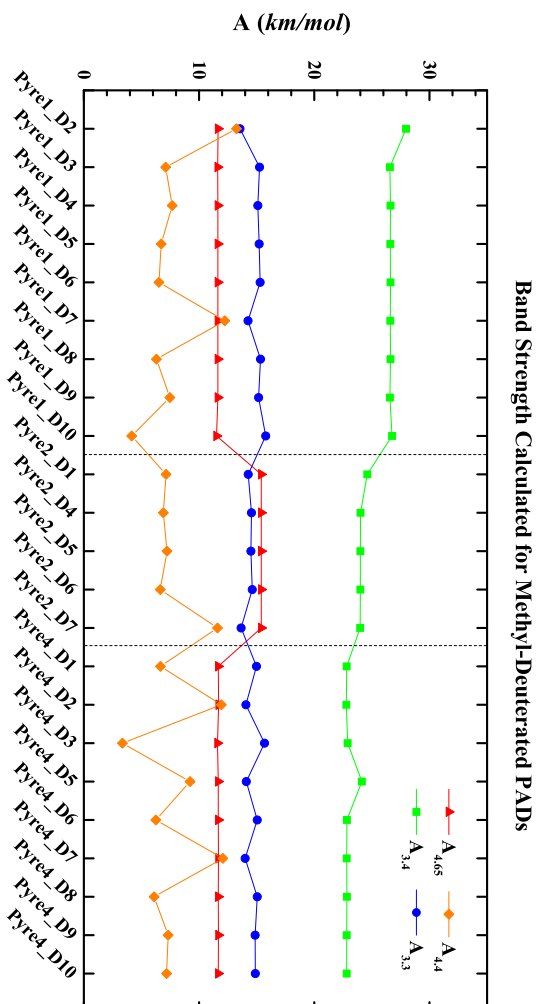


Fig. 13.— Same as Figure 7 but for pyrenes containing a methyl-deuterated sidegroup as well as a peripheral D atom.

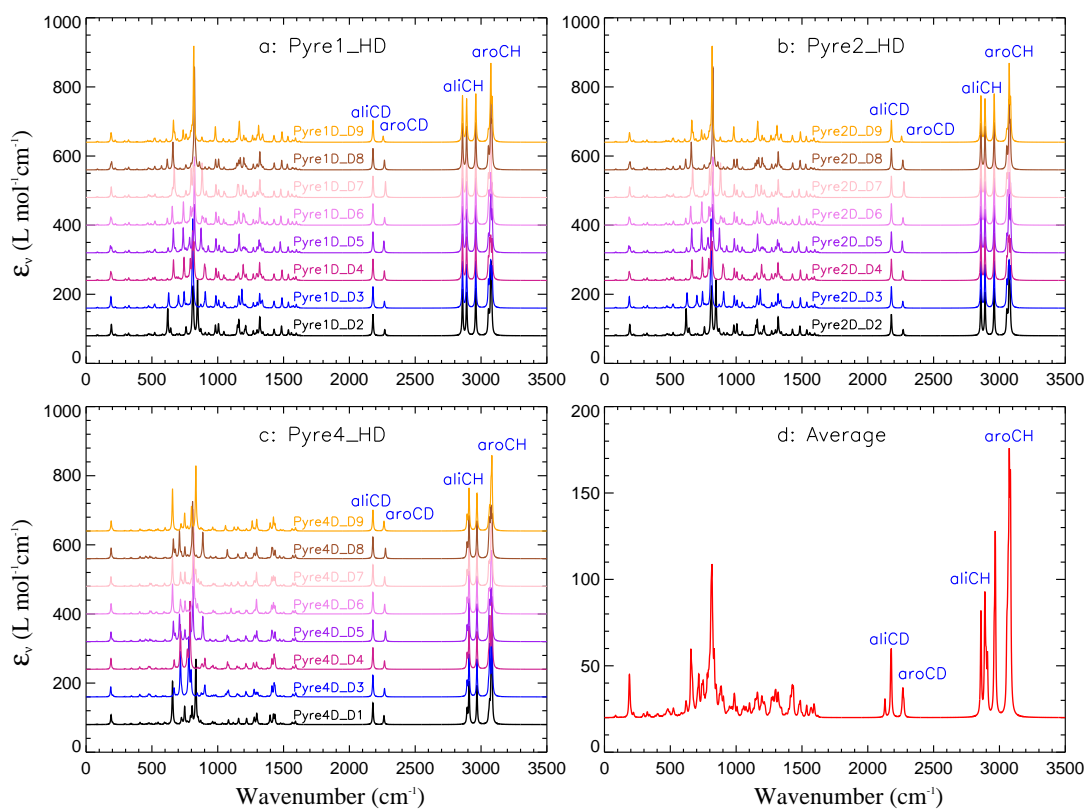


Fig. 14.— Same as Figure 6 but for “superdeuterated” pyrenes containing an H+H pair, an H+D pair, as well as a peripheral D atom (see Figure 5).

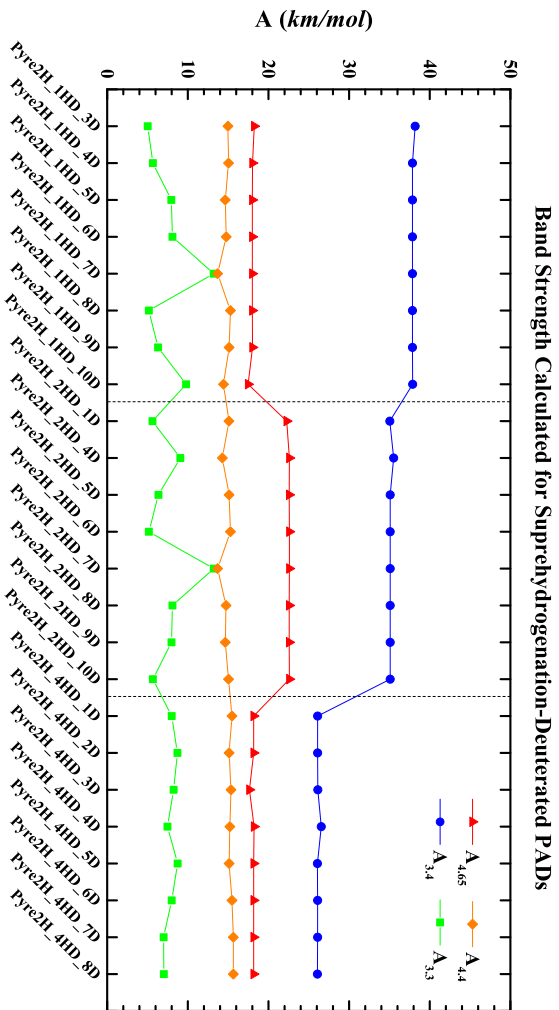


Fig. 15.— Same as Figure 7 but for “superdeuterated” pyrenes containing an H+H pair, an H+D pair, as well as a peripheral D atom.

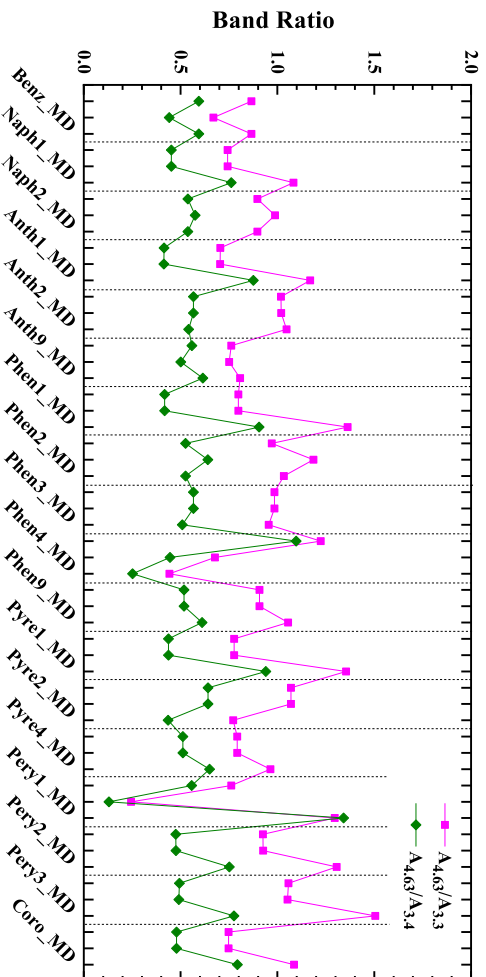


Fig. 16.— Band-strength ratios of $A_{4,65}/A_{3,3}$ (magenta) and $A_{4,65}/A_{3,4}$ (green) for methyl-deuterated PAHs (see Figure 1).

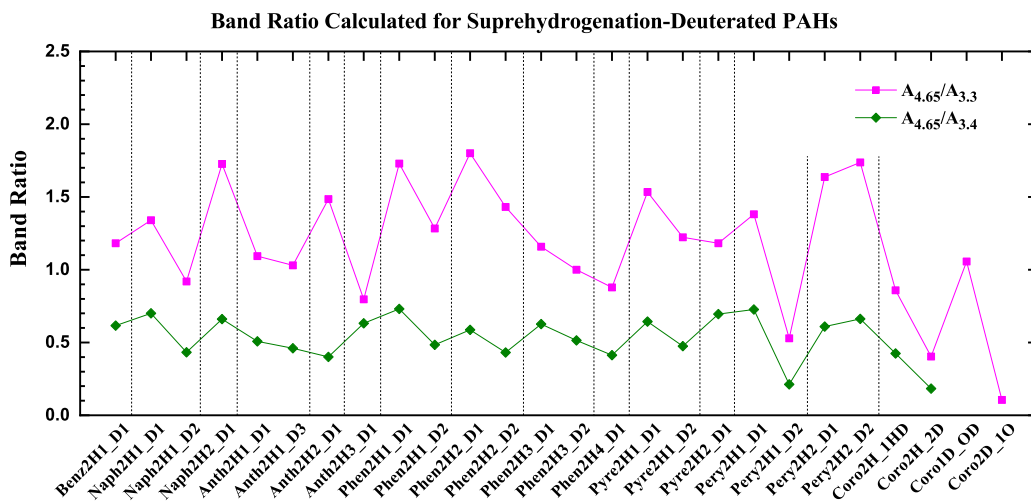


Fig. 17.— Band-strength ratios of $A_{4.65}/A_{3.3}$ (magenta) and $A_{4.65}/A_{3.4}$ (green) for “superdeuterated” PAHs in which one H atom and one D atom share an C atom (see Figure 2).

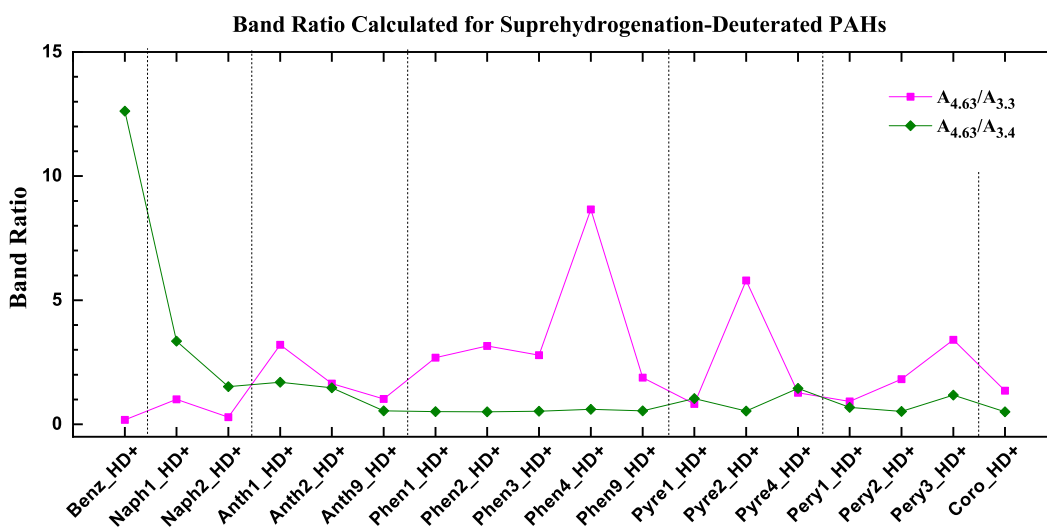


Fig. 18.— Band-strength ratios of $A_{4.65}/A_{3.3}$ (magenta) and $A_{4.65}/A_{3.4}$ (green) for “superdeuterated” PAH cations (see Figure 3).

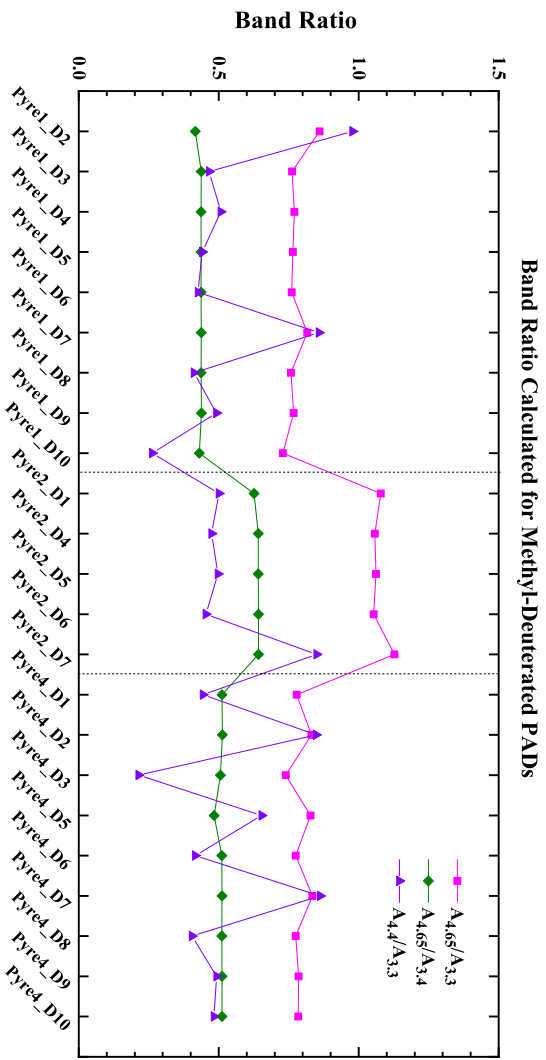


Fig. 19.— Band-strength ratios of $A_{4.65}/A_{3.3}$ (magenta), $A_{4.65}/A_{3.4}$ (green), and $A_{4.4}/A_{3.3}$ (blue) for pyrenes containing a methyl-deuterated sidegroup as well as a peripheral D atom (see Figure 4).

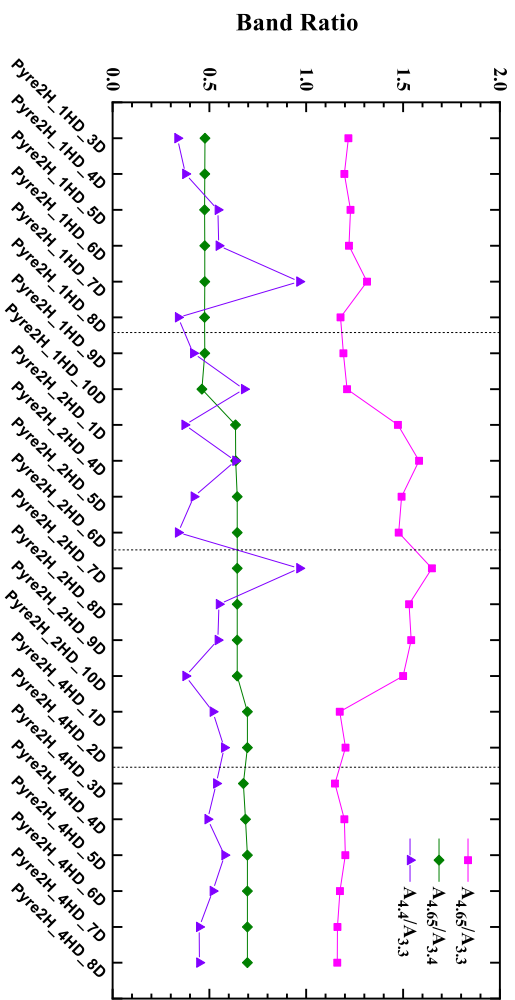


Fig. 20.— Band-strength ratios of $A_{4.65}/A_{3.3}$ (magenta), $A_{4.65}/A_{3.4}$ (green), and $A_{4.4}/A_{3.3}$ (blue) for "superdeuterated" pyrenes containing an H+H pair, an H+D pair, as well as a peripheral D atom (see Figure 5).

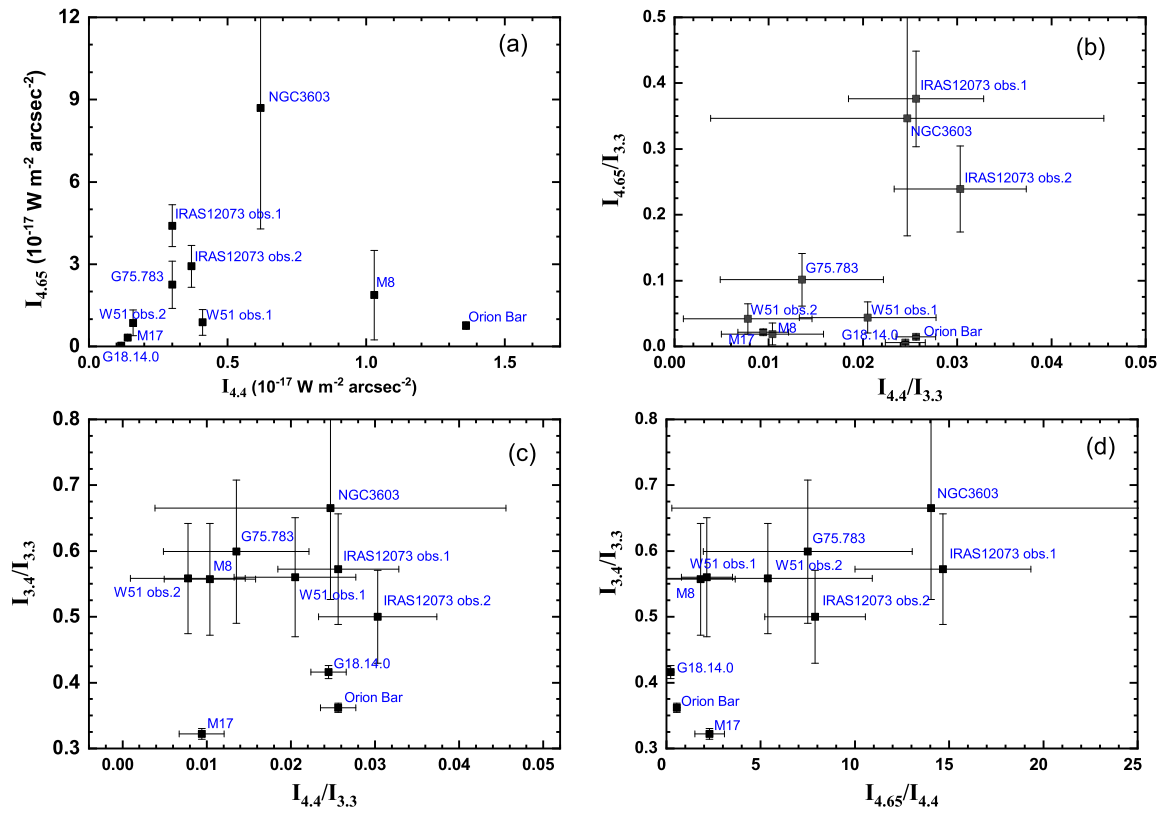


Fig. 21.— Upper left (a): Correlation of the observed intensities of the $4.65 \mu\text{m}$ aliphatic C–D band ($I_{4.65}$) with that of the $4.4 \mu\text{m}$ aromatic C–D band ($I_{4.4}$). Upper right (b): Correlation of $I_{4.65}/I_{3.3}$ with $I_{4.4}/I_{3.3}$. Bottom left (c): Correlation of $I_{3.4}/I_{3.3}$ with $I_{4.4}/I_{3.3}$. Bottom right (d): Correlation of $I_{3.4}/I_{3.3}$ with $I_{4.65}/I_{4.4}$.

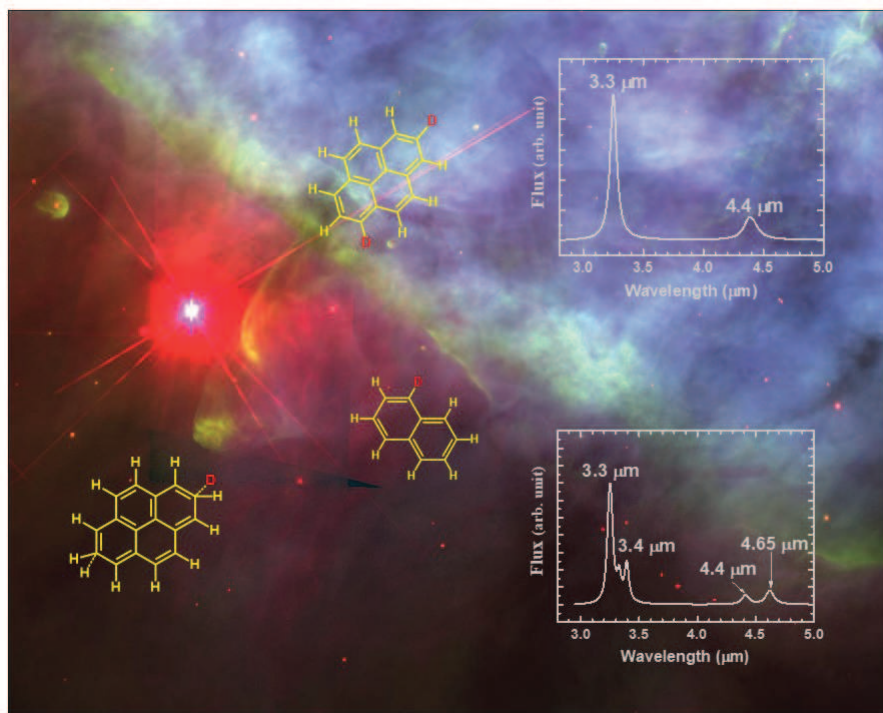


Fig. 22.— Schematic illustration of the deuteration of PAHs in the Orion Bar PDR, from regions near the ionization front where the C–D bonds are mostly aromatic, to regions intermediate between the ionization front and the dissociation front where PAHs could be superhydrogenated and even superdeuterated.

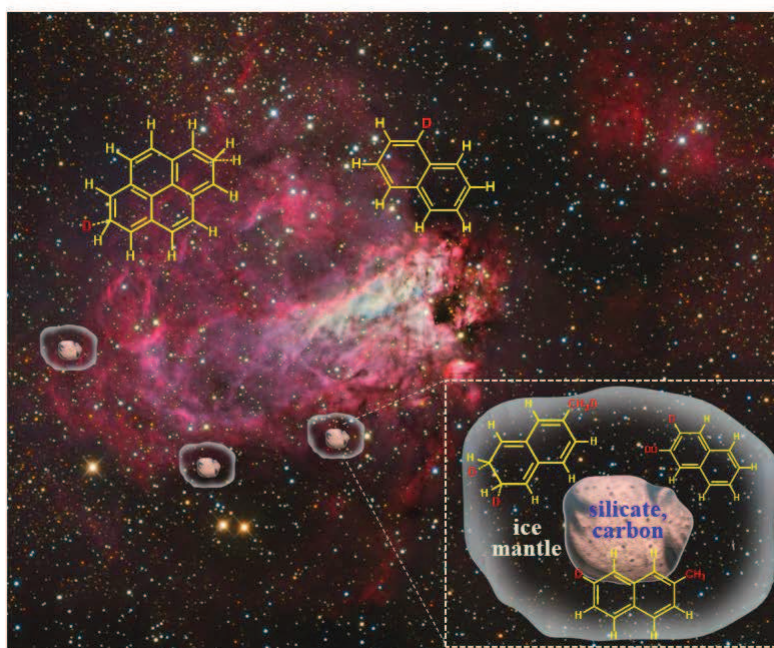


Fig. 23.— Schematic illustration of the deuteration of PAHs in the M17 dense molecular cloud. The deuteration occurs in the UV irradiated, D-enriched ice mantles coated on dust grains and generates aliphatic C–D units.

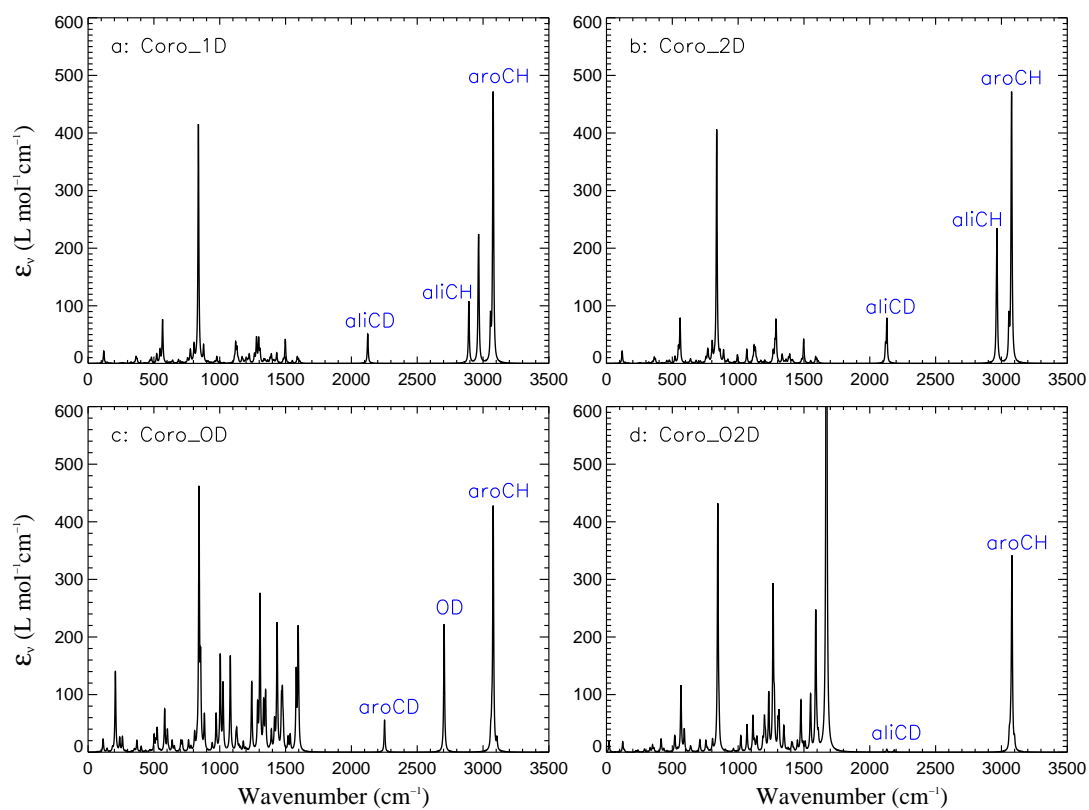


Fig. 24.— Vibrational spectra of “superdeuterated” coronene (a), doubly “superdeuterated” coronene (b), and deuterated, oxidized coronenes (c, d).

Table 1: Wavelengths (λ) and Intensities (A_λ in km mol^{-1}) of the Nominal “3.3 μm ” Aromatic C–H Stretch, “3.4 μm ” Aliphatic C–H Stretch and “4.65 μm ” Aliphatic C–D Stretch Computed at the B3LYP/6-311+G** Level for All the Methyl-Deuterated PAHs Shown in Figure 1.

Compound	$\lambda_{3.3}$ (μm)	$A_{3.3}$ (km mol^{-1})	$\lambda_{3.4}$ (μm)	$A_{3.4}$ (km mol^{-1})	$\lambda_{4.65}$ (μm)	$A_{4.65}$ (km mol^{-1})	$A_{4.65}/A_{3.3}$
Benz_CH ₂ D	3.25	14.42	3.37	21.29	4.60	11.53	0.80
Naph_CH ₂ D	3.25	13.88	3.37	22.58	4.60	12.37	0.89
Anth_CH ₂ D	3.25	13.82	3.37	22.24	4.59	12.28	0.89
Phen_CH ₂ D	3.24	13.07	3.37	22.64	4.59	12.43	0.95
Pyre_CH ₂ D	3.25	14.66	3.38	23.93	4.60	13.62	0.93
Pery_CH ₂ D	3.25	13.73	3.38	24.38	4.60	13.73	1.00
Coro_CH ₂ D	3.25	16.58	3.38	24.83	4.60	14.24	0.86
Average	3.25	14.31	3.37	23.13	4.60	12.89	0.90
stdev	0.00	1.12	0.00	1.28	0.00	0.98	0.07

Table 2: Wavelengths (λ) and Intensities (A_λ in km mol^{-1}) of the Nominal “3.3 μm ” Aromatic C–H Stretch, “3.4 μm ” Aliphatic C–H Stretch and “4.65 μm ” Aliphatic C–D Stretch Computed at the B3LYP/6-311+G** Level for All the “Supedeuterated” PAHs Shown in Figure 2.

Compound	$\lambda_{3.3}$ (μm)	$A_{3.3}$ (km mol^{-1})	$\lambda_{3.4}$ (μm)	$A_{3.4}$ (km mol^{-1})	$\lambda_{4.65}$ (μm)	$A_{4.65}$ (km mol^{-1})	$A_{4.65}/A_{3.3}$
Benz_HD	3.26	16.47	3.43	32.84	4.67	17.82	1.08
Naph_HD	3.25	14.69	3.42	32.39	4.70	19.32	1.31
Anth_HD	3.25	14.47	3.43	28.88	4.66	15.98	1.10
Phen_HD	3.25	13.59	3.42	32.29	4.66	17.82	1.31
Pyre_HD	3.25	15.07	3.42	32.18	4.62	17.69	1.17
Pery_HD	3.24	13.71	3.43	33.05	4.65	17.82	1.30
Coro_HD	3.27	17.24	3.40	37.89	4.71	6.97	0.40
Average	3.25	15.03	3.42	32.79	4.66	16.20	1.10
Stdev	0.01	1.36	0.01	2.65	0.03	4.18	0.32

Table 3: Wavelengths (λ) and Intensities (A_λ in km mol^{-1}) of the Nominal “3.3 μm ” Aromatic C–H Stretch, “3.4 μm ” Aliphatic C–H Stretch “4.65 μm ” Aliphatic C–D Stretch Computed at the B3LYP/6-311+G** Level for All the “Superdeuterated” PAH Cations Shown in Figure 3.

Compound	$\lambda_{3.3}$ (μm)	$A_{3.3}$ (km mol^{-1})	$\lambda_{3.4}$ (μm)	$A_{3.4}$ (km mol^{-1})	$\lambda_{4.65}$ (μm)	$A_{4.65}$ (km mol^{-1})	$A_{4.65}/A_{3.3}$
Benz_HD+	3.24	9.01	3.31	0.13	4.81	1.61	0.18
Naph_HD+	3.22	0.84	3.51	0.22	4.66	0.64	0.76
Anth_HD+	3.24	1.32	3.51	2.28	4.79	2.23	1.68
Phen_HD+	3.23	0.33	3.49	2.15	4.75	1.18	3.56
Pyre_HD+	3.24	0.46	3.50	1.39	4.78	0.95	2.09
Pery_HD+	3.22	1.10	3.51	2.74	4.78	2.27	2.07
Coro_HD+	3.23	1.92	3.48	5.20	4.75	2.62	1.36
Average	3.23	2.14	3.47	2.02	4.76	1.64	1.67
Stdev	0.01	3.08	0.07	1.73	0.05	0.75	1.00

Table 4: Wavelengths (λ) and Intensities (A_λ in km mol^{-1}) of the Nominal “3.3 μm ” Aromatic C–H Stretch, “3.4 μm ” Aliphatic C–H Stretch, “4.4 μm ” Aromatic C–D Stretch and “4.65 μm ” Aliphatic C–D Stretch Computed at the B3LYP/6-311+G** Level for Deuterated Pyrenes Containing a Methyl-Deuterated Sidegroup as well as a Periphral D Atom Shown in Figure 4.

Compound	$\lambda_{3.3}$ (μm)	$A_{3.3}$ (km mol^{-1})	$\lambda_{3.4}$ (μm)	$A_{3.4}$ (km mol^{-1})	$\lambda_{4.4}$ (μm)	$A_{4.4}$ (km mol^{-1})	$\lambda_{4.65}$ (μm)	$A_{4.65}$ (km mol^{-1})	$A_{4.65}/A_{3.3}$
Pyre1_D1	3.25	15.30	3.37	26.61	4.41	6.52	4.62	11.63	0.76
Pyre1_D2	3.25	15.79	3.37	26.75	4.38	4.15	4.62	11.51	0.73
Pyre1_D3	3.25	15.16	3.37	26.57	4.41	7.46	4.62	11.64	0.77
Pyre1_D4	3.25	15.10	3.37	26.61	4.41	7.67	4.62	11.63	0.77
Pyre1_D5	3.25	13.54	3.37	27.97	4.42	13.25	4.62	11.65	0.86
Pyre1_D6	3.25	15.25	3.37	26.56	4.41	7.11	4.62	11.62	0.76
Pyre1_D7	3.25	15.21	3.37	26.61	4.41	6.71	4.62	11.63	0.76
Pyre1_D8	3.25	14.25	3.37	26.59	4.40	12.23	4.62	11.63	0.82
Pyre1_D9	3.25	15.34	3.37	26.61	4.41	6.31	4.62	11.63	0.76
Pyre2_D1	3.26	14.62	3.38	23.99	4.41	6.65	4.57	15.39	1.05
Pyre2_D4	3.26	14.56	3.38	24.00	4.41	6.96	4.57	15.35	1.05
Pyre2_D5	3.25	14.40	3.38	24.02	4.43	7.72	4.57	14.91	1.04
Pyre2_D6	3.26	14.51	3.38	23.99	4.41	7.22	4.57	15.39	1.06
Pyre2_D7	3.26	13.65	3.38	23.99	4.40	11.60	4.57	15.39	1.13
Pyre4_D1	3.25	15.05	3.37	22.84	4.41	6.26	4.62	11.67	0.78
Pyre4_D2	3.25	14.88	3.37	22.81	4.41	7.19	4.62	11.67	0.78
Pyre4_D3	3.25	14.87	3.37	22.82	4.41	7.32	4.62	11.68	0.79
Pyre4_D4	3.25	15.68	3.37	22.90	4.37	3.36	4.62	11.60	0.74
Pyre4_D5	3.25	14.10	3.37	24.13	4.43	9.22	4.62	11.67	0.83
Pyre4_D6	3.25	14.00	3.37	22.82	4.40	12.06	4.62	11.68	0.83
Pyre4_D7	3.25	15.05	3.37	22.83	4.41	6.09	4.62	11.67	0.78
Pyre4_D8	3.25	14.99	3.37	22.81	4.41	6.66	4.62	11.67	0.78
Pyre4_D9	3.25	14.07	3.37	22.78	4.40	11.93	4.62	11.69	0.83
average	3.25	14.76	3.37	24.68	4.41	7.90	4.61	12.43	0.85
stdev	0.00	0.61	0.00	1.80	0.01	2.60	0.02	1.54	0.12

Table 5: Wavelengths (λ) and Intensities (A_λ in km mol^{-1}) of the Nominal “3.3 μm ” Aromatic C–H Stretch, “3.4 μm ” Aliphatic C–H Stretch, “4.4 μm ” Aromatic C–D Stretch and “4.65 μm ” Aliphatic C–D Stretch Computed at the B3LYP/6-311+G** Level for All the “Superdeuterated” Pyrenes Containing an H+H Pair, an H+D Pair, as well as a Periphral D Atom. Shown in Figure 5.

Compound	$\lambda_{3.3}$ (μm)	$A_{3.3}$ (km mol^{-1})	$\lambda_{3.4}$ (μm)	$A_{3.4}$ (km mol^{-1})	$\lambda_{4.4}$ (μm)	$A_{4.4}$ (km mol^{-1})	$\lambda_{4.65}$ (μm)	$A_{4.65}$ (km mol^{-1})	$A_{4.65}/A_{3.3}$
Pyre1D_D1	3.26	15.29	3.44	37.86	4.41	5.17	4.59	18.00	1.18
Pyre1D_D2	3.26	15.06	3.44	37.86	4.41	5.66	4.59	18.02	1.20
Pyre1D_D3	3.26	14.65	3.44	37.86	4.41	7.96	4.59	18.00	1.23
Pyre1D_D4	3.25	14.43	3.44	37.89	4.42	9.79	4.59	17.47	1.21
Pyre1D_D5	3.26	15.13	3.44	37.86	4.41	6.31	4.59	18.03	1.19
Pyre1D_D6	3.26	13.70	3.44	37.85	4.40	13.22	4.59	18.00	1.31
Pyre1D_D7	3.25	14.76	3.44	37.86	4.41	8.09	4.59	18.01	1.22
Pyre1D_D8	3.25	14.97	3.44	38.19	4.43	5.01	4.59	18.23	1.22
Pyre2D_D1	3.26	15.28	3.45	35.10	4.41	5.16	4.60	22.58	1.48
Pyre2D_D2	3.26	15.05	3.45	35.09	4.41	5.67	4.60	22.59	1.50
Pyre2D_D3	3.26	14.65	3.45	35.09	4.41	7.96	4.60	22.58	1.54
Pyre2D_D4	3.25	14.28	3.44	35.52	4.42	9.06	4.60	22.60	1.58
Pyre2D_D5	3.26	15.13	3.45	35.09	4.41	6.35	4.60	22.58	1.49
Pyre2D_D6	3.26	13.69	3.45	35.09	4.40	13.21	4.60	22.59	1.65
Pyre2D_D7	3.25	14.75	3.45	35.09	4.41	8.10	4.60	22.58	1.53
Pyre2D_D8	3.25	15.11	3.45	35.05	4.43	5.61	4.60	22.25	1.47
Pyre4D_D1	3.25	15.20	3.41	26.54	4.42	7.47	4.59	18.20	1.20
Pyre4D_D2	3.25	15.65	3.41	26.08	4.41	7.01	4.59	18.16	1.16
Pyre4D_D3	3.25	15.64	3.41	26.09	4.41	7.00	4.59	18.17	1.16
Pyre4D_D4	3.25	15.11	3.41	26.08	4.40	8.74	4.59	18.16	1.20
Pyre4D_D5	3.25	15.47	3.41	26.09	4.41	8.00	4.59	18.16	1.17
Pyre4D_D6	3.25	15.48	3.41	26.08	4.41	8.01	4.59	18.16	1.17
Pyre4D_D7	3.25	15.11	3.41	26.09	4.40	8.71	4.59	18.17	1.20
Pyre4D_D8	3.25	15.36	3.41	26.12	4.42	8.23	4.59	17.64	1.15
Average	3.25	14.96	3.43	33.06	4.41	7.73	4.59	19.54	1.31
Stdev	0.00	0.52	0.02	5.13	0.01	2.16	0.00	2.18	0.17

Table 6: *Mean* Intensities of the 3.3 μm Aromatic C–H Stretch ($A_{3.3}$) and the 4.65 μm Aliphatic C–D Stretch ($A_{4.65}$) Computed at the B3LYP/6-311+G** Level for All the Deuterated PAHs Considered in This Work. The $A_{3.3}$ and $A_{4.65}$ Band Strengths Are on a Per C–H or C–D Bond Basis.

Band Strengths	Neutral PAHs	Cationic PAHs
$A_{3.3}$ (km mol^{-1})	14.76 ± 0.33	$2.14^{+3.08}_{-2.14}$
$A_{4.65}$ (km mol^{-1})	15.26 ± 3.31	1.64 ± 0.75
$A_{4.65}/A_{3.3}$	1.04 ± 0.21	1.67 ± 1.00

Table 7: A Summary of the Power Emitted from the $3.3\ \mu\text{m}$ Aromatic C–H Stretch $(I_{3.3})_{\text{obs}}$, the $3.4\ \mu\text{m}$ Aliphatic C–H Stretch $(I_{3.4})_{\text{obs}}$, the $4.4\ \mu\text{m}$ Aromatic C–D Stretch $(I_{4.4})_{\text{obs}}$, and the $4.65\ \mu\text{m}$ Aliphatic C–D Stretch $(I_{4.65})_{\text{obs}}$ Compiled from Astronomical Observations. Also Shown Are the Degree of Deuteration Derived for Each Source

Object	Type	aromatic C–H		aliphatic C–H		aromatic C–D			aliphatic C–D		
		$(I_{3.3})_{\text{obs}}^{\dagger}$	$(I_{3.4})_{\text{obs}}^{\dagger}$	$(I_{3.4}/I_{3.3})_{\text{obs}}^{\dagger}$	f_{aliCH}	$(I_{4.4})_{\text{obs}}^{\dagger}$	$(I_{4.4}/I_{3.3})_{\text{obs}}^{\dagger}$	f_{aroCD}	$(I_{4.65})_{\text{obs}}^{\dagger}$	$(I_{4.65}/I_{3.3})_{\text{obs}}^{\dagger}$	f_{aliCD}
G75.78+0.34 ^a	HII Region	22.2 ± 2.0	13.3 ± 2.1	59.9 ± 4.1	34.0 ± 4.7	0.30 ± 0.19	1.35 ± 0.73	3.3 ± 1.3	2.25 ± 0.86	10.1 ± 2.96	7.1 ± 4.1
NGC3603 ^a	HII Region	25.1 ± 2.4	16.7 ± 3.1	66.5 ± 6.0	37.8 ± 5.7	0.62 ± 0.52	2.47 ± 1.84	5.9 ± 2.8	8.70 ± 4.41	34.7 ± 14.3	20.6 ± 16.0
W51 obs.1 ^a	HII Region	20.0 ± 1.8	11.2 ± 1.5	56.0 ± 2.5	31.8 ± 4.0	0.41 ± 0.14	2.05 ± 0.52	5.0 ± 1.5	0.88 ± 0.47	4.40 ± 1.95	3.2 ± 2.1
W51 obs.2 ^a	HII Region	20.6 ± 1.8	11.5 ± 1.4	55.8 ± 1.9	31.7 ± 3.9	0.16 ± 0.14	0.78 ± 0.61	1.9 ± 0.9	0.86 ± 0.47	4.17 ± 1.92	3.0 ± 2.0
M8 ^a	HII Region	99.1 ± 8.9	55.2 ± 6.8	55.7 ± 1.9	31.6 ± 3.9	1.03 ± 0.53	1.04 ± 0.44	2.6 ± 0.9	1.87 ± 1.63	1.89 ± 1.48	1.4 ± 1.3
IRAS112073 obs.1 ^a	HII Region	11.7 ± 1.0	6.7 ± 0.8	57.3 ± 1.9	32.5 ± 4.0	0.30 ± 0.08	2.56 ± 0.46	6.1 ± 1.8	4.40 ± 0.76	37.6 ± 3.28	22.0 ± 13.1
IRAS112073 obs.2 ^a	HII Region	12.2 ± 1.0	6.1 ± 0.7	50.0 ± 1.6	28.4 ± 3.5	0.37 ± 0.08	3.03 ± 0.41	7.2 ± 2.1	2.92 ± 0.76	23.9 ± 4.27	15.2 ± 8.8
M17b ^a	PDR	12.3 ± 1.5	6.6 ± 1.8	53.7 ± 8.1	30.5 ± 5.9	--	--	--	3.32 ± 1.94	27.0 ± 12.5	16.8 ± 13.2
M17 ^b	PDR	14.9 ± 0.2	4.8 ± 0.1	32.2 ± 0.2	18.3 ± 2.2	0.14 ± 0.04	0.94 ± 0.26	2.3 ± 0.7	0.32 ± 0.06	2.15 ± 0.37	1.6 ± 0.8
Orion Bar ^b	PDR	53.1 ± 0.6	19.2 ± 0.3	36.2 ± 0.2	20.5 ± 2.5	1.36 ± 0.11	2.56 ± 0.18	6.1 ± 1.7	0.76 ± 0.13	1.43 ± 0.23	1.1 ± 0.5
G18.14.0 ^b	Reflection Nebula	4.78 ± 0.06	1.99 ± 0.04	41.6 ± 0.3	23.7 ± 2.8	0.12 ± 0.01	2.45 ± 0.18	5.9 ± 1.6	0.03 ± 0.01	0.56 ± 0.20	0.4 ± 0.2

[†] Flux densities in units of $10^{-17}\ \text{W m}^{-2}\ \text{arcsec}^{-2}$

^a Doney et al. 2016

^b Onaka et al. 2014